Commun Nonlinear Sci Numer Simulat 128 (2024) 107647

Contents lists available at ScienceDirect

Communications in Nonlinear Science and Numerical Simulation

journal homepage: www.elsevier.com/locate/cnsns

Research paper

Double-Hopf bifurcation and Pattern Formation of a Gause-Kolmogorov-Type system with indirect prey-taxis and direct predator-taxis

Dongxu Geng [a,*], Hao Wang [b,c], Weihua Jiang [d], Hongbin Wang [d]

[a] School of Science, Nanjing University of Posts and Telecommunications, Nanjing, 210003, China
[b] Interdisciplinary Lab for Mathematical Ecology & Epidemiology, AB T6G 2G1, Canada
[c] Department of Mathematical and Statistical Sciences, University of Alberta, AB T6G 2G1, Canada
[d] School of Mathematics, Harbin Institute of Technology, Harbin 150001, China

ARTICLE INFO

Keywords:
Double-Hopf bifurcation
Spatiotemporal pattern
Predator-prey system
Indirect prey-taxis
Spatially nonhomogeneous
Quasi-periodic solution

ABSTRACT

This paper focuses on a general Gause-Kolmogorov-Type predator–prey model with direct predator-taxis and indirect prey-taxis. The global existence and boundedness of solutions to the system are proved. Our approach is applicable to more general situation. Some measures of success for the constant coexistence steady state are rigorously calculated, such as decreasing the indirect prey-taxis sensitivity or the release rate of stimulus, and increasing the predator-taxis sensitivity or the decay rate of stimulus. By choosing the indirect prey-taxis coefficient as the bifurcation parameter, the existence of Hopf and double-Hopf bifurcations is established. We find that both indirect prey-taxis and direct predator-taxis can promote the complexity of the spatiotemporal pattern, e.g. spatially nonhomogeneous periodic patterns with different spatial frequency, spatially nonhomogeneous quasi-periodic patterns. Finally, we apply our theoretical analyses to a Rosenzweig–MacArthur model with indirect prey-taxis and direct predator-taxis, spatially homogeneous periodic patterns.

1. Introduction

Predator-prey interaction is a fundamental relationship between species in an ecosystem. To model this interaction with movement, random diffusion has been widely used to describe "drunk" animals' movement, with the implicit assumption that the movements of predator and prey species move randomly like a particle. A simple derivation uses Fick's law of diffusion. The long term dynamics of such models were fully investigated [1–5]. A variety of classical reaction–diffusion models [6,7] have been built up to illustrate the spatial patchy structure of species even in a homogeneous environment. Cognitive movement is a key feature of animals in contrast to chemical movement as extensively discussed in Wang and Salmaniw [8], and it provides an effective mechanism to interpret the spatiotemporal patchy distribution of species, for example, see the studies on memory-based diffusion in single species [9–11] or predator–prey [12]. Prey-taxis (predators pursue prey) and predator-taxis (prey escape from predators) are cognitive movement mechanisms in a predator–prey system. These taxis can be derived from a modified Fick's law and strongly regulate the spatiotemporal dynamics and patterns of predator–prey interaction [13–18].

* Corresponding author at: School of Science, Nanjing University of Posts and Telecommunications, Nanjing, 210003, China.
E-mail address: geng_dx@163.com (D. Geng).

https://doi.org/10.1016/j.cnsns.2023.107647
Received 30 July 2023; Received in revised form 15 October 2023; Accepted 19 October 2023
Available online 28 October 2023

The following predator–prey models with prey-taxis or predator-taxis have been extensively studied:

$$\begin{cases} N_t = d_N \triangle N + F(N) - \phi(N,P), & x \in \Omega,\ t > 0, \\ P_t = d_P \triangle P - \eta \nabla \cdot (P \nabla N) + e\phi(N,P) - g(P), & x \in \Omega,\ t > 0, \end{cases} \tag{1.1}$$

and

$$\begin{cases} N_t = d_N \triangle N + \xi \nabla \cdot (N \nabla P) + F(N) - \phi(N,P), & x \in \Omega,\ t > 0, \\ P_t = d_P \triangle P + e\phi(N,P) - g(P), & x \in \Omega,\ t > 0. \end{cases} \tag{1.2}$$

The prey-taxis model (1.1) was first proposed by Karevia and Odell [16] based on some experimental observations, and further interpreted by Othmer and Stevens [19] stating "The purposes of taxis range from movement toward food and avoidance of noxious substances to large-scale aggregations for survival". The necessary conditions of pattern formation for a variety of non-linear functional responses have been established in [15]. Considering a smooth bounded domain, the existence and uniqueness of classical solutions of system(1.1) was obtained in [20]. The global bifurcation and pattern formations of system (1.1) were investigated in [21]. For a more general form of system (1.1), the global existence and boundedness of solutions were proved in [17] with the existence of a global attractor, the uniform persistence, and the global stability of the positive equilibrium for some special prey growth and functional responses via a Lyapunov function. The predator-taxis model (1.2) was studied in [18] for the global existence and boundedness of solutions in bounded domains. The incorporation of predator-taxis can eliminate diffusion-induced instability and make the constant steady state regain its stability. A model with both prey-taxis and predator-taxis was explored in [22] for the impact of these taxis on spatial patterns.

As noted in [23,24], direct prey-taxis cannot reproduce stable spatially heterogeneous dynamics. In some scenarios, indirect prey-taxis takes over, that is, the predator moves perceptually according to stimulus emitted by prey such as specific odor, pheromones, exometabolites, scent marks [24,25]. Many predator–prey systems consist of tiny prey and large predators, such as army ants and anteater, such that prey can directly judge the predator's location while predators cannot easily see prey's location. Therefore, it is reasonable to assume direct predator-taxis and indirect prey-taxis as follows:

$$\begin{cases} N_t = d_N \triangle N + \xi \nabla \cdot (N \nabla P) + N f(N) - P g(N), & x \in \Omega,\ t > 0, \\ P_t = d_P \triangle P - \eta \nabla \cdot (P \nabla S) + e P g(N) - mP, & x \in \Omega,\ t > 0, \\ S_t = d_S \triangle S + \alpha N - \beta S, & x \in \Omega,\ t > 0, \end{cases} \tag{1.3}$$

where $N(x,t)$, $P(x,t)$ are the respective densities of prey and predator populations at space location x and time t, $g(N)$ is the functional response function of predation and $Pg(N)$ measures the predation rate, $f(N)$ represents the per-capita growth rate of prey. The parameters m and e are the mortality rate and conversion efficiency of the predator, respectively, and the parameters d_N, d_P are corresponding diffusion coefficients of the prey and predator species. Moreover, the predator-taxis term $\xi \nabla \cdot (N \nabla P)$ describes the tendency of prey moving away from the predator with the rate $\xi \geq 0$. The indirect prey-taxis term $-\eta \nabla \cdot (P \nabla S)$ with the rate $\eta \geq 0$ describes the tendency of the predator moving toward stimulus emitted by prey, where $S(x,t)$ represents the taxis stimulus concentration. All other parameters are assumed to be positive constants.

Given $\xi = 0$, the system (1.3) only has indirect prey-taxis, which has been studied in the literature. Ignoring the self-dissipation of stimulus, i.e. $\beta = 0$, the critical bifurcation values of the taxis coefficient were determined by Routh–Hurwitz criterion in [26], which also explored pattern formation and chaos. A PDE of the predator with indirect prey-taxis coupled with an ODE of prey was analyzed in [27]. Indirect prey-taxis can lead to interesting spatial patterns [28]. The authors generalized some existing results derived for particular cases of taxis models. Moreover, the global existence and uniform boundedness of solutions was proved for general functional responses in [29], which showed that prey-taxis plays an essential role in pattern formation. An indirect prey-taxis model with Allee effect in the predator population was considered in [30]. Their results suggested that the prey–taxis movement of the predator can induce various spatially nonhomogeneous patterns via the destabilization of the constant steady state and spatially homogeneous periodic solutions. In particular, indirect prey-taxis allows the predator overcoming the Allee effect for persistence. Recently, the system (1.3) with $\xi = 0$ was studied in [31], which determined the existence of Hopf, Turing, Turing–Hopf and double-Hopf bifurcations. By calculating the normal form of double-Hopf bifurcation, the authors showed stable spatially homogeneous and nonhomogeneous periodic solutions, as well as stable spatially nonhomogeneous quasi-periodic solutions near the double-Hopf bifurcation point. The results illustrated that spatially nonhomogeneous Hopf bifurcations can be induced by indirect prey-taxis, which is impossible to be generated by direct prey-taxis.

In this paper, we will investigate the system (1.3) with homogeneous Neumann boundary conditions on a smooth bounded spatial domain:

$$\begin{cases} N_t = d_N \triangle N + \xi \nabla \cdot (N \nabla P) + N f(N) - P g(N), & x \in \Omega,\ t > 0, \\ P_t = d_P \triangle P - \eta \nabla \cdot (P \nabla S) + e P g(N) - mP, & x \in \Omega,\ t > 0, \\ S_t = d_S \triangle S + \alpha N - \beta S, & x \in \Omega,\ t > 0, \\ \frac{\partial N}{\partial \nu} = \frac{\partial P}{\partial \nu} = \frac{\partial S}{\partial \nu} = 0, & x \in \partial\Omega,\ t > 0, \\ N(x,0) = N_0(x) \geq 0, \quad P(x,0) = P_0(x) \geq 0, \quad S(x,0) = S_0(x) \geq 0, & x \in \Omega, \end{cases} \tag{1.4}$$

where Ω is chosen as $(0, l\pi)$ with l being a positive constant. In (1.4), $Nf(N)$ represents the prey growth rate, which is typically negative for large N because of the crowding effect, for instance,

$$\text{Logistic}: \quad Nf(N) = aN\left(1 - \frac{N}{K}\right), \quad \text{Allee}: \quad Nf(N) = aN\left(1 - \frac{N}{K}\right)\left(\frac{N}{G} - 1\right), \tag{1.5}$$

where $a > 0$, $0 < G < K$. The functional response of predation $g(N)$ takes the following forms:

$$\text{type II}: \quad g(N) = \frac{\gamma N}{b+N}, \quad \text{type III}: \quad g(N) = \frac{\gamma N^n}{b^n + N^n}. \tag{1.6}$$

Reasonably we assume $f(N)$ and $g(N)$ satisfy the following conditions:

(H1) $f : [0,\infty) \to \mathbb{R}$ is continuously differentiable and there exists positive constants C_f^1, C_f^2 such that $f(N) \le C_f^1 - C_f^2 N$ for any $N \ge 0$;

(H2) $g : [0,\infty) \to [0,\infty)$ is continuously differentiable and there exist positive constants C_g such that $g(N) \le C_g$ for any $N \ge 0$.

For the systems with only direct prey-taxis or direct predator-taxis, the global existence and uniform boundedness of solutions have been well studied [17,18]. Global well-posedness and stability analyses for the systems with only indirect prey-taxis [29] or indirect predator-taxis [32] are discussed as well. However, little work was done for the global solvability of the system (1.3) with both direct predator-taxis and indirect prey-taxis. Recently, for the predator–prey system with prey taxis, repulsive chemotaxis and predator evasion have been considered in [33] and blow up solutions in finite time have been found for the space dimension $n = 2$ by numerical simulations. For a general reaction–diffusion predator–prey model with indirect prey-taxis and indirect predator-taxis, the global existence and uniformly boundedness of the classical solution have been proved for spatial dimension $n \le 3$ under some conditions, see [34]. Therefore in this paper, we will first prove the global existence and uniform boundedness of solutions to (1.3) for space dimension $n = 1$, based on the literature [8], we will also study measures of success for the system (1.4) focusing on the tendencies between prey and predator, and the emission and decay of stimulus. In addition, we present thorough bifurcation analysis with details provided below. We find that Turing bifurcations cannot occur for the system (1.4) by considering the natural scenario of attractive indirect prey-taxis. We establish the existence conditions of Hopf bifurcations and double-Hopf bifurcations, which can induce spatially homogeneous and spatially nonhomogeneous periodic solutions, and even spatially nonhomogeneous quasi-periodic solutions through the secondary bifurcation of double-Hopf bifurcation. It is worth noting that double-Hopf bifurcation is impossible to occur for the system with direct prey-taxis and predator-taxis, and only Hopf bifurcation of the spatially homogeneous periodic solution can occur. Thus we can assert that indirect prey-taxis can promote complex spatiotemporal patterns.

The remaining paper is organized as follows. In Section 2, we prove the global existence and uniform boundedness of the solution to (1.4) by combining semigroup estimates with Moser-Alikakos iteration method. Subsequently, some measures of success for the constant coexistence steady state are presented in Section 3. In Section 4, thorough bifurcation analysis are provided with proofs, including Hopf, Turing and double-Hopf bifurcations, and the stability of the positive constant steady state is determined. In Section 5, we apply our theory to a Rosenzweig–MacArthur model with indirect prey-taxis and direct predator-taxis, and numerical simulations illustrate and complement our theoretical results. Finally, we summarize our work in Section 6. To this end, we use $\|\cdot\|_p$ as the norm of the space L^p for $p \in [1,\infty]$, $\|\cdot\|_{k,p}$ as the norm of the space $W^{k,p}$ for $k = 1,2, p \in [1,\infty]$, and denote $\mathbb{N}$ the set of all positive integers, and $\mathbb{N}_0 := \mathbb{N} \cup \{0\}$.

2. Global existence

2.1. Local existence and preliminaries

In this section, we first show the local existence of solutions to system (1.3) such that the problem is well-posed at least locally. Following the abstract theory of quasilinear parabolic systems in [35], we illustrate the local-in-time existence result of a classical solution to (1.3).

Lemma 2.1. *Assume that $\Omega \subset \mathbb{R}^n$, is a smooth bounded domain, the conditions **(H1)** and **(H2)** hold, then for any initial data $(N_0, P_0, S_0) \in (W^{1,p}(\Omega))^3$ for $p > n$, $N_0 \ge 0, P_0 \ge 0, S_0 \ge 0$, the following statements hold:*

(i) *There exists a positive constant T_{max} such that the system (1.4) has a unique non-negative classical solution$(N(x,t), P(x,t), S(x,t))$ satisfying*

$$(N,P,S) \in (C(0,T_{max}); W^{1,p}(\Omega)) \cap C^{2,1}(\Omega \times (0,T_{max}))^3.$$

(ii) *N, P, S satisfy $N(x,t) \ge 0, P(x,t) \ge 0, S(x,t) \ge 0$, and there exist positive constants C_1, C_2, C_3 such that the total mass of N, P, S satisfy*

$$\int_\Omega N(x,t)dx \le C_1, \quad \int_\Omega P(x,t)dx \le C_2, \quad \int_\Omega S(x,t)dx \le C_3, \tag{2.1}$$

for all $t \in [0,T_{max}]$, where $C_1 := max\{\|N_0\|_1, \frac{C_f^1|\Omega|}{C_f^2}\}$, $C_2 := max\{e\|N_0\|_1 + \|P_0\|_1, \frac{e(m+C_f^1)C_1}{m}\}$, $C_3 := max\{\|S_0\|_1, \frac{\alpha C_1}{\beta}\}$.

(iii) *If for any $T > 0$, there exists a constant $M(T)$ depending on T such that*

$$\|N(\cdot,t)\|_\infty + \|P(\cdot,t)\|_\infty + \|S(\cdot,t)\|_\infty < M(T), \ t \in [0, \ T],$$

then $T_{max} = +\infty$.

Proof. Let $U = (N, P, S)$, then the system (1.3) can be rewritten as

$$\begin{cases} U_t = \nabla \cdot (a(U)\nabla U) + \Phi(U), & x \in \Omega,\ t > 0, \\ \frac{\partial U}{\partial \nu} = 0, & x \in \partial\Omega,\ t > 0, \\ U(\cdot, 0) = (N_0, P_0, S_0), & x \in \Omega, \end{cases} \tag{2.2}$$

where

$$a(U) = \begin{pmatrix} d_N & \xi N & 0 \\ 0 & d_P & -\eta P \\ 0 & 0 & d_S \end{pmatrix}, \quad \Phi(U) = \begin{pmatrix} Nf(N) - Pg(N) \\ ePg(N) - mP \\ \alpha N - \beta S \end{pmatrix}.$$

Obviously, the system (2.2) is uniformly parabolic since real parts of all the eigenvalues are positive, thus the local existence of $(N(x,t), P(x,t), S(x,t))$ in part (i) can be derived directly by [35, Theorem 14.4, 14.6]. Obviously, $a(U)$ in (2.2) is a upper triangular matrix, and it can be equivalent to a lower triangular by elementary transformations, then by [36, Theorem 15.5], we have $T_{max} = +\infty$, which completes the proof of the part (iii).

To prove part (ii), we rewrite the first equation of (1.3) as

$$\begin{cases} N_t = d_N \triangle N + \xi \nabla N \nabla P + \xi N \triangle P + Nf(N) - Pg(N), & x \in \Omega,\ t > 0, \\ \frac{\partial N}{\partial \nu} = 0, & x \in \partial\Omega,\ t > 0, \\ N(x, 0) = N_0(x) \geq 0, & x \in \Omega. \end{cases} \tag{2.3}$$

The Eq. (2.3) can be treated as a scalar linear equation of N, and it is obvious that $\underline{N} = 0$ is a lower solution to (2.3), then we obtain $N(x,t) \geq 0$ by applying the maximum principle for parabolic equations. Similarly, we can prove $P(x,t) \geq 0$ and $S(x,t) \geq 0$. Next we will show that the solution $(N(x,t), P(x,t), S(x,t))$ is L^1-bounded. Let

$$\int_\Omega N(x,t)dx = Q_1(t), \quad \int_\Omega P(x,t)dx = Q_2(t), \quad \int_\Omega S(x,t)dx = Q_3(t),$$

integrating the N-equation of (1.3), by the assumption **(H1)**, we have

$$\frac{dQ_1(t)}{dt} = \int_\Omega Nf(N) - Pg(N)dx \leq \int_\Omega C_f^1 N - C_f^2 N^2 dx, \tag{2.4}$$

following Hölder's inequality, we know that

$$\int_\Omega N^2 dx \geq \frac{1}{|\Omega|}\left(\int_\Omega N dx\right)^2. \tag{2.5}$$

Plugging (2.5) to (2.4) and treating (2.4) as a ODE of $Q_1(t)$, we obtain

$$\int_\Omega N(x,t)dx = Q_1(t) < C_1, \tag{2.6}$$

where $C_1 = \max\{\|N_0\|_1, \frac{C_f^1|\Omega|}{C_f^2}\}$.

Next, combining the first and second equations of (1.3) and integrating over Ω leads to

$$\begin{aligned}(eQ_1(t) + Q_2(t))_t &= e\int_\Omega Nf(N)dx - m\int_\Omega Pdx \leq eC_f^1 \int_\Omega Ndx - m\int_\Omega Pdx \\ &\leq -m(eQ_1(t) + Q_2(t)) + e(m + C_f^1)C_1,\end{aligned}$$

then in the similar manner to (2.4), we obtain

$$eQ_1(t) + Q_2(t) \leq \max\{e\|N_0\|_1 + \|P_0\|_1, \frac{e(m + C_f^1)C_1}{m}\} := C_2,$$

which implies

$$\int_\Omega P(x,t)dx = Q_2(t) \leq C_2.$$

Finally, by (2.6) we obtain the boundedness of S in $L^1(\Omega)$:

$$\int_\Omega S(x,t)dx \leq \max\{\|S_0\|_1, \frac{\alpha C_1}{\beta}\} := C_3. \quad \square$$

Next, we will review some well-known results on preliminary estimates in [37], which will play a key role in our proof of global solvability of (1.4).

According to [37,38], for $p \in (1, \infty)$, we can define the sectorial operator A by

$$Au := -\triangle u \text{ for } u \in D(A) := \{\varphi \in W^{2,p}(\Omega) : \frac{\partial \varphi}{\partial \nu} = 0, \text{ on } \partial\Omega\}.$$

The operator $A+1$ is also sectorial in $L^p(\Omega)$ and the fractional operator $(A+1)^\theta, 0 < \theta < 1$ is defined on $D((A+1)^\theta) \subset L^p(\Omega)$ satisfying

$$\|u\|_{D((A+1)^\theta)} := \|(A+1)^\theta u\|_{L^p(\Omega)} < \infty,$$

and the domain has the embedding property:

$$D((A+1)^{\theta}) \hookrightarrow W^{1,p}(\Omega),$$

Similarly, we can define A_d given by $A_d u = -d \triangle u$, which satisfies the same properties as A, hence we only state the results on A here and A_d follows a direct scaling. Now we recall some smoothing $L^p - L^q$ type estimates for the diffusion semigroup with homogeneous Neumann boundary conditions on a bounded, smooth domain, refer to [33,37,38].

Lemma 2.2.

(i) *Assume that* $k \in \{0,1\}$, $1 \le p \le \infty$, $1 < q < \infty$. *There exists a constant* $c_1 > 0$, *such that*

$$\|u\|_{k,p} \le c_1 \|(A+1)^{\theta} u\|_q, \tag{2.7}$$

for any $u \in D((A+1)^{\theta})$ *with* $0 < \theta < 1$ *satisfying*

$$k - \frac{n}{p} < 2\theta - \frac{n}{q}.$$

If additionally for any $u \in L^{q'}(\Omega)$, $q \ge q'$, *then there exists* $c_2 > 0$, $r > 0$ *such that*

$$\|(A+1)^{\theta} e^{-t(A+1)} u\|_q \le c_2 (t^{-\theta - \frac{n}{2}(\frac{1}{p} - \frac{1}{q})}) e^{-rt} \|u\|_{q'}, \tag{2.8}$$

where $e^{-t(A+1)}$ *maps* $L^{q'}$ *into* $D((A+1)^{\theta})$.

(ii) *For* $1 < p < \infty$, *there exist some positive constants* c_3, $\epsilon > 0$ *and* μ, *such that*

$$\|(A+1)^{\theta} e^{-tA} \nabla \cdot u\|_p \le c_3 (t^{-\theta - \frac{1}{2} - \epsilon}) e^{-\mu t} \|u\|_p, \tag{2.9}$$

for all $u \in L^p$.

The following lemma states the Gagliardo–Nirenberg inequality,refer to [39–41], that will be applied to prove the boundedness of $N(x,t), P(x,t)$ in the next subsection.

Lemma 2.3. *There exists an constant* $C_{GN} > 0$ *such that*

$$\|u\|_p \le C_{GN} \|u\|_{1,q}^{\sigma} \|u\|_k^{1-\sigma}, \tag{2.10}$$

for $u \in W^{1,q}(\Omega)$, *where* $p \ge q \ge 1$, $p \ge k$ *satisfy*

$$\frac{\frac{n}{k} - \frac{n}{p}}{1 + \frac{n}{k} - \frac{n}{q}} \le \sigma \le 1$$

with sharply inequality if $k = 1$ *or* $q = 1$.

Via direct applying the result in [37, Lemma 2.1] to the system (1.4), we can obtain the following conclusion which estimates the $L^p(\Omega)$ boundedness of S by using corresponding $L^1(\Omega)$ bounds.

Lemma 2.4. *Assume that there exist* $\tau \in (0, \min\{1, T_{max}\})$ *and a positive integer* $\gamma \in [1,n]$, *such that*

$$\|N(t)\|_{\gamma} \le C_1, \quad \text{for all } t \in [\tau, T_{max}).$$

Then for any $\eta \in (0, T_{max} - \tau)$, *the following estimation holds*

$$\|S(t)\|_{1,p} \le c(p, \max\{\|N_0\|_1, \|S_0\|_1\}, \tau, \eta)(1 + C_1) \quad \text{for all } t \in [\tau + \eta, T_{max}), \tag{2.11}$$

for all $1 < p < \frac{n\gamma}{n-\gamma}$.

2.2. Global existence and uniform boundedness

In this section, we will prove the global existence and uniform boundedness of the solution to (1.4) for the spatial dimension $n = 1$. It is noting that a series of standard semigroup arguments are well-established to prove the uniform boundedness of the solution for the system with taxis in the literature, refer to [18,37,38,42,43]. Another approach is the iterative technique of Moser and Alikakos [44,45], it also can be employed to obtain such L^{∞}-boundedness. In the present paper, due to that N, P, S-equations in the system (1.4) are coupled with each other, in order to simplify the proof process as much as possible, we have to combine the above two approaches to prove some expected results.

Firstly, we employ the semigroup argument to obtain $S \in W^{1,p}(\Omega)$ for any $1 < p < \infty$, then combining with the embedding theorem, the L^{∞}-boundedness of S can be derived.

Lemma 2.5. *Let* (N, P, S) *be a classical solution to the system* (1.4) *in* $(0, T_{max})$, *then there exists a positive constant* M_1 *such that for each* $p \in (1, \infty)$,

$$\|S(\cdot,t)\|_{1,p} < M_1, \quad \text{for all } t \in (0, T_{max}). \tag{2.12}$$

Proof. First, we prove there exists a $M(\tau) > 0$ such that

$$\|S(\cdot,t)\|_{1,p} < M(\tau), \quad \text{for } t \in (\tau, T_{max}).$$

It follows Lemma 2.1-(ii) that

$$\|N(t)\|_1 \le C_1,$$

choose $\tau \in (0, \min\{1, T_{max}\})$, $p > 1$ and $\gamma = 1$, then by Lemma 2.4, for any $\eta \in (0, T_{max} - \tau)$, the following estimation holds

$$\|S(t)\|_{1,p} \le c(p, \tau, \eta, \max\{\|N_0\|_1, \|S_0\|_1\})(1 + C_1) \quad \text{for all } t \in [\tau + \varepsilon, T_{max}),$$

for all $1 < p < \infty$, here c is an constant depending on $p, \tau, \varepsilon, \|N_0\|_1, \|S_0\|_1$.

Let $\varepsilon \to 0$, we derive that for each $1 < p < \infty$,

$$\|S(\cdot,t)\|_{1,p} \le M(\tau), \tag{2.13}$$

for all (τ, T_{max}), here $M(\tau)$ is a constant that depends on τ. Since (2.13) holds for any $\tau \in (0, \min\{1, T_{max}\})$, and $S_0 \in W^{1,p}$, hence we infer that there exists a constant M_1 independing of t, such that for $1 < p < \infty$,

$$\|S(\cdot,t)\|_{1,p} < M_1, \quad \text{for all } \ t \in (0, T_{max}). \quad \square$$

Since

$$W^{1,p}(\Omega) \hookrightarrow L^\infty(\Omega), \quad \text{for } 1 < p < \infty,$$

so we also know

$$\|S(\cdot,t)\|_\infty < M_1, \quad \text{for all } \ t \in (0, T_{max}). \tag{2.14}$$

Next we will establish the uniform boundedness of $P(x,t)$. To avoid the tedious process of proving $P \in L^k(\Omega)$ needed in semigroup theory to obtain the uniform boundedness, we will employ Moser-Alikakos iterative technique here together with Lemma 2.5.

Lemma 2.6. *Let (N, P, S) be a classical solution to the system (1.4) in $(0, T_{max})$, then there exists a positive constant M_2 such that for each $1 < p < \infty$,*

$$\|P(\cdot,t)\|_{1,p} < M_2, \quad \textit{for all } t \in (0, T_{max}). \tag{2.15}$$

Proof. By multiplying the P-equation by $P(\cdot,t)$ and integrating on Ω, Combining the assumption **(H2)** we obtain

$$\begin{aligned}
\frac{1}{2}\frac{d}{dt}\int_\Omega P^2 dx &= \int_\Omega P P_t dx \\
&= d_P \int_\Omega P \vartriangle P dx - \eta \int_\Omega P \nabla \cdot (P \nabla S) dx + \int_\Omega P(eP g(N) - mP) dx \\
&\le -d_P \int_\Omega |\nabla P|^2 dx + \eta \int_\Omega P \nabla P \nabla S dx + eC_g \int_\Omega P^2 dx - m \int_\Omega P^2 dx,
\end{aligned}$$

then we have

$$\frac{1}{2}\frac{d}{dt}\int_\Omega P^2 dx + d_P \int_\Omega |\nabla P|^2 dx + m \int_\Omega P^2 dx \le \eta \int_\Omega P \nabla P \nabla S dx + eC_g \int_\Omega P^2 dx, \tag{2.16}$$

Via Young inequality and Hölder's inequality, we know that

$$\begin{aligned}
\int_\Omega P \nabla P \nabla S dx &\le \varepsilon_0 \int_\Omega |\nabla P|^2 dx + C(\varepsilon_0) \int_\Omega P^2 |\nabla S|^2 dx \\
&\le \varepsilon_0 \int_\Omega |\nabla P|^2 dx + C(\varepsilon_0) \left(\int_\Omega P^4\right)^{\frac{1}{2}} \left(\int_\Omega |\nabla S|^4\right)^{\frac{1}{2}} dx \\
&:= \varepsilon_0 \int_\Omega |\nabla P|^2 dx + C(\varepsilon_0) \|P\|_4^2 \|\nabla S\|_4^2.
\end{aligned} \tag{2.17}$$

here $\varepsilon_0 > 0$. According to Lemma 2.3, we derive Gagliardo–Nirenberg inequality for $p = 4, q = 2, n = k = 1, \sigma = \frac{1}{2}$

$$\|P\|_4^2 < C_{GN}^2 \|P\|_{1,2} \|P\|_1, \tag{2.18}$$

Owing to (2.1), (2.12), (2.18) and Young inequality, that there exists a sufficiently small $\varepsilon_1 > 0$, such that

$$\begin{aligned}
C(\varepsilon_0)\|P\|_4^2 \|\nabla S\|_4^2 &\le \varepsilon_1 (\|P\|_2^2 + \|\nabla P\|_2^2) + C(\varepsilon_1) \left(C(\varepsilon_0) C_{GN}^2 \|P\|_1 \|\nabla S\|_4^2\right)^2 \\
&\le \varepsilon_1 (\|P\|_2^2 + \|\nabla P\|_2^2) + K_0,
\end{aligned} \tag{2.19}$$

where K_0 is dependent of $\varepsilon_0, \varepsilon_1, C_{GN}$, C_2 and M_1.

On the other hand, it follows Lemma 2.3 and Poincaré inequality that for any $\varepsilon_2 > 0$, such that

$$\int_\Omega P^2 dx \le \varepsilon_2 \int_\Omega |\nabla P|^2 dx + C(\varepsilon_2)\left(\int_\Omega P dx\right)^2. \tag{2.20}$$

Therefore following (2.17), (2.19) and (2.20), we have

$$\begin{aligned}\eta \int_\Omega P\nabla P\nabla S dx + eC_g \int_\Omega P^2 dx \le& \varepsilon_0\eta \int_\Omega |\nabla P|^2 + \varepsilon_1\eta\left(\int_\Omega P^2 dx + \int_\Omega |\nabla P|^2 dx\right) + eC_g\int_\Omega P^2 dx \\ &+ \eta K_0 \\ \le& (\varepsilon_0+\varepsilon_1)\eta \int_\Omega |\nabla P|^2 dx + \eta K_0 \\ &+ (eC_g + \varepsilon_1\eta)\left(\varepsilon_2 \int_\Omega |\nabla P|^2 dx + C(\varepsilon_2)\left(\int_\Omega P dx\right)^2\right).\end{aligned} \tag{2.21}$$

Choose $\varepsilon_0 = \varepsilon_1 = \frac{d_P}{4\eta}$, $\varepsilon_2 = \frac{d_P}{2(\varepsilon_1\eta + eC_g)}$, then based on (2.16) we obtain the following inequality

$$\frac{d}{dt}\int_\Omega P^2 dx + 2m\int_\Omega P^2 dx \le K_1,$$

where K_1 is positive constant depending on e, η, d_P, C_g and K_0. Then we get

$$\|P(\cdot,t)\|_2 \le \max\{\|P_0\|_2, \frac{K_1}{2m}\}. \tag{2.22}$$

By the variation of constants formula for the second equation of (1.4), we obtain

$$\begin{aligned}P(\cdot,t) =& e^{-t(A_{d_P}+1)}P_0 - \eta\int_0^t e^{-(t-s)(A_{d_P}+1)}\nabla\cdot(P(\cdot,t)\nabla S(\cdot,t))ds \\ &+ \int_0^t e^{-(t-s)(A_{d_P}+1)}\psi(N(\cdot,t),P(\cdot,t),x)ds \\ &:= I_1 + I_2 + I_3,\end{aligned} \tag{2.23}$$

where $\psi(N(\cdot,t),P(\cdot,t),x) := eP(\cdot,t)g(N(\cdot,t)) + (1-m)P(\cdot,t)$. Taking a sufficiently small constant $\tau \in (0, \min\{1, T_{max}\})$, then we will estimate I_1, I_2, I_3 are L_∞ bounded by applying Lemma 2.2 based on (2.22).

For I_1, we fix $k = 0, p = \infty$ in (2.7), then

$$\|I_1\|_\infty \le c_1\|(A_{d_S}+1)^\theta e^{-t(A_{d_S}+1)}P_0\|_q \le C_5\tau^{-\theta}e^{-rt}\|P_0\|_q \le C_5\|P_0\|_\infty := M_1(\tau), \tag{2.24}$$

for all $t \in (\tau, T_{max})$, $\theta \in (\frac{1}{2q}, 1)$, where C_5 is a positive constant.

For I_2, according to (2.9), there additionally exists constants $\epsilon \in (0, \frac{1}{2}-\theta)$ and $C_6 > 0$ such that for $q = 2$, $\theta \in (\frac{1}{2q}, \frac{1}{2})$

$$\begin{aligned}\|I_2\|_\infty \le& c_1\eta\int_0^t e^{-(t-s)}\|(A_{d_P}+1)^\theta e^{-(t-s)A_{d_P}}\nabla\cdot(P(\cdot,t)\nabla S(\cdot,t))\|_q ds \\ \le& C_6\int_0^t (t-s)^{-\theta-\frac{1}{2}-\epsilon}e^{-(\mu+1)(t-s)}\|P(\cdot,t)\nabla S(\cdot,t)\|_q ds,\end{aligned} \tag{2.25}$$

for all $t \in (0, T_{max})$. By (2.12) and (2.22), we know that there exists a positive constant C_7 such that

$$\|P(\cdot,t)\nabla S(\cdot,t)\|_2 < C_7 \quad \text{for } t \in (\tau, T_{max}), \tag{2.26}$$

hence there exists a constant $C_8 > 0$ such that

$$\begin{aligned}\|I_2\|_\infty \le& C_6C_7\int_0^t (t-s)^{-\theta-\frac{1}{2}-\epsilon}e^{-(\mu+1)(t-s)}ds \\ \le& C_8\Gamma(\frac{1}{2}-\theta-\epsilon), \quad \text{for } t \in (\tau, T_{max}),\end{aligned} \tag{2.27}$$

where $\Gamma(x)$ represents Gamma function and since $\frac{1}{2}-\theta-\epsilon > 0$, then $\Gamma(\frac{1}{2}-\theta-\epsilon) > 0$.

Finally for I_3, we take $q' = q = 2$, $\theta \in (\frac{1}{4}, 1)$

$$\begin{aligned}\|I_3\|_\infty \le& c_1c_2\int_0^t (t-s)^{-\theta}e^{-r(t-s)}\|\psi(N(\cdot,t),P(\cdot,t),x)\|_q ds \\ \le& C_9\int_0^t (t-s)^{-\theta}e^{-r(t-s)}\|(eC_g+1-m)P(\cdot,t)\|_q ds \\ \le& C_9\Gamma(1-\theta),\end{aligned} \tag{2.28}$$

where C_9 is a constant that could be different between lines, $\Gamma(1-\theta) > 0$ for $1-\theta > 0$. Therefore, by (2.24), (2.27), and (2.28), we obtain P is uniformly bounded, i.e.

$$\|P(\cdot,t)\|_\infty \le C_4 \tag{2.29}$$

holds for any $t \in (0, T_{max})$ since $\|P_0\| < \infty$.

Furthermore, we can prove the $W^{1,p}$ boundedness of P based on (2.12) and (2.29). Concretely, also taking $\tau \in (0, \min\{1, T_{max}\})$, for $k = 1, n = 1$, $q = q' > p$ and $\theta \in (\frac{1}{2}(1 - \frac{n}{p} + \frac{n}{q}), 1)$. Then via utilizing the similar arguments to the proofs of (2.24), (2.27), and (2.28), the following consequence is derived

$$\|P\|_{1,p} \le \|I_1\|_{1,p} + \|I_2\|_{1,p} + \|I_3\|_{1,p} \le \infty, \quad \text{for all } t \in \{\tau, T_{max}\}$$

Since $P_0 \in W^{1,p}$ for all $p > n$, thus let $\tau \to 0$, we obtain there exists a constant M_2, such that

$$\|P\|_{1,p} \le M_2, \quad \text{for all } t \in (0, T_{max}) \quad \Box$$

Corollary 2.7. *Let (N, P, S) be a classical solution to the system (1.4) in $(0, T_{max})$, then there exists a positive constant M_3 such that*

$$\|N(\cdot,t)\|_\infty < M_3, \quad \textit{for all } t \in (0, T_{max}). \tag{2.30}$$

Proof. For any $k \ge 2$, multiplying the N-equation by $N(\cdot,t)$, from the assumption **(H1)** we obtain

$$\begin{aligned}\frac{d}{dt}\int_\Omega N^k dx &= -d_N k(k-1)\int_\Omega N^{k-2}|\nabla N|^2 dx - \xi k(k-1)\int_\Omega N^{k-1}\nabla N \nabla P dx\\ &\quad + k\int_\Omega N^{k-1}(Nf(N) - Pg(N))dx\\ &\le -d_N \frac{4(k-1)}{k}\int_\Omega |\nabla N^{\frac{k}{2}}|^2 dx + 2\xi(k-1)\int_\Omega N^{\frac{k}{2}}\nabla N^{\frac{k}{2}}\nabla P dx\\ &\quad + kC_f^1\int_\Omega N^k dx - kC_f^2\int_\Omega N^{k+1}dx\end{aligned} \tag{2.31}$$

Applying the Hölder's inequality to the second term of (2.31), we arrive at

$$\int_\Omega N^{\frac{k}{2}}\nabla N^{\frac{k}{2}}\nabla P dx \le \left(\int_\Omega N^{k+1}dx\right)^{\frac{k}{2(k+1)}}\left(\int_\Omega |\nabla N^{\frac{k}{2}}|^2\right)^{\frac{1}{2}}\left(\int_\Omega |\nabla P|^{2(k+1)}\right)^{\frac{1}{2(k+1)}}, \tag{2.32}$$

plugging it into (2.31), and using (2.15) and Young inequality with $\epsilon = \frac{2d_N}{\xi k}$, we derive

$$\frac{d}{dt}\int_\Omega N^k dx \le K\left(\int_\Omega N^{k+1}dx\right)^{\frac{k}{k+1}} + kC_f^1\int_\Omega N^k dx - kC_f^2\int_\Omega N^{k+1}dx \tag{2.33}$$

with K depending on k, M_2. On the other hand, Young inequality leads to

$$K\left(\int_\Omega N^{k+1}dx\right)^{\frac{k}{k+1}} \le \epsilon\int_\Omega N^{k+1}dx + C_\epsilon K^{k+1}, \tag{2.34}$$

and Hölder's inequality leads to

$$\left(\int_\Omega N^k dx\right)^{\frac{k+1}{k}} \le K'\int_\Omega N^{k+1}dx. \tag{2.35}$$

Through taking $\epsilon = \frac{kC_f^2}{2}$, and plugging (2.34) and (2.35) into (2.33), we have

$$\frac{d}{dt}\int_\Omega N(\cdot,t)^k dx \le kC_f^1\int_\Omega N(\cdot,t)^k dx + C_\epsilon K^{k+1} - \frac{kC_f^2}{2K'}\left(\int_\Omega N(\cdot,t)^k dx\right)^{\frac{k+1}{k}}.$$

Denoting the following differential equation

$$\frac{dy}{dt} \le -\alpha_1 y^\kappa + \alpha_2 y + \alpha_0.$$

where $y(t) := \int_\Omega N(\cdot,t)^k dx$, $\kappa = \frac{k+1}{k}$, $\alpha_1 = \frac{kC_f^2}{2K'}$, $\alpha_2 = kC_f^1$, $\alpha_0 = C_\epsilon K^{k+1}$. We know

$$y(t) \le \max\{y(0), \bar{y}\}, \tag{2.36}$$

here $\bar{y}$ is the solution of $-\alpha_1 y^\kappa + \alpha_2 y + \alpha_0 = 0$. Therefore, for any $k \ge 2$,

$$\|N(\cdot,t)\|_k < \infty. \quad \Box \tag{2.37}$$

Thus based on (2.15) and (2.37), by applying Lemma 2.2 again, the $W^{1,p}$ boundedness of N can be derived through the similar argument as the proof of Lemma 2.6, furthermore, following embedding theorem, we have that there exists a constant M_3, such that

$$\|N(\cdot,t)\|_\infty < M_3, \quad \text{for all } t \in (0, T_{max}).$$

As a consequence, the main results on the global existence of the classical solution to (1.3) can be derived by combining Lemma 2.1-(iii) with Lemmas 2.5, 2.6 and Corollary 2.7.

Theorem 2.8. *Let $\Omega \in \mathbb{R}$ be a bounded domain with smooth boundary. Assume that d_N, d_P, d_S, $e, m > 0$, $\xi, \eta \geq 0$, $f(N)$ and $g(N)$ satisfy the conditions* **(H1)**, **(H2)**. *Then for any initial data $(N_0, P_0, S_0) \in (W^{1,p}(\Omega))^3$ for $p > 1$, $N_0 \geq 0, P_0 \geq 0, S_0 \geq 0$, the system (1.4) possesses a unique global classical solution (N, P, S) satisfying*

$$(N, P, S) \in (C(0,\infty); W^{1,p}(\Omega)) \cap C^{2,1}(\Omega \times (0,\infty))^3, \tag{2.38}$$

which is uniformly bounded in $\Omega \times (0,\infty)$, i.e. there is a constant $M(N_0, P_0, S_0) > 0$ such that

$$\|N(\cdot,t)\|_\infty + \|P(\cdot,t)\|_\infty + \|S(\cdot,t)\|_\infty < M(N_0, P_0, S_0), \quad \textit{for all } t \in (0,\infty). \tag{2.39}$$

3. Measures of success

The direct taxis (simulated visually and acoustically) or indirect taxis (simulated by chemosensation) considered in the model (1.4) guide cognitive movement of animals. As illustrated in [8], one of the quantitative success measures for animal movement models with population dynamics combines growth rates and survival to determine the optimal diffusion and flow rate of the pattern. A successful strategy makes the population persisting the stability as $t \to \infty$ and an unsuccessful one drives the population to go unstable. As a result, this section will seek the successful or unsuccessful strategy by analyzing the eigenvalue problem of (1.4) at the constant coexistence state.

We propose the following hypotheses:

(H3) $g(N)$ satisfies $g'(N) > 0$, $g(0) = 0$ and there a exist positive constant N^* such that $g(N^*) = \frac{m}{e}$.

Such hypotheses assure the system (1.4) possesses an unique positive equilibrium, denoted by $E^* = (N^*, P^*, S^*)$, where

$$N^* := g^{-1}\left(\frac{m}{e}\right), \quad P^* := \frac{m}{e} N^* f(N^*), \quad S^* := \frac{\alpha}{\beta} N^*. \tag{3.1}$$

The linearized the system (1.4) at (N^*, P^*, S^*) is given by

$$\begin{cases} N_t = d_N \triangle N + \xi N^* \triangle P + N(f(N^*) + N^* f'(N^*) - P^* g'(N^*)) - g(N^*)P, \\ P_t = d_P \triangle P - \eta P^* \triangle S + eP^* g'(N^*)N + P(eg(N^*) - m), \\ S_t = d_S \triangle S + \alpha N - \beta S, \\ \frac{\partial N}{\partial \nu} = \frac{\partial N}{\partial \nu} = \frac{\partial N}{\partial \nu} = 0, \end{cases} \tag{3.2}$$

for $x \in (0, l\pi)$, $t > 0$. Denote that

$$D = \begin{pmatrix} d_N & \xi N^* & 0 \\ 0 & d_P & -\eta P^* \\ 0 & 0 & d_S \end{pmatrix}, \tag{3.3}$$

$$J = \begin{pmatrix} a_{11} & -g(N^*) & 0 \\ eP^* g'(N^*) & 0 & 0 \\ \alpha & 0 & -\beta \end{pmatrix}, \tag{3.4}$$

where

$$a_{11} = f(N^*) + N^* f'(N^*) - P^* g'(N^*). \tag{3.5}$$

Then we generalize the linearized system (3.2) to obtain

$$\frac{\partial U}{\partial t} = D \triangle U + J(U(x,t)), \tag{3.6}$$

where $U(x,t) = (N(x,t), P(x,t), S(x,t))$, $x \in \Omega$, N^*, P^*, S^* are defined in (3.1), D and J refer to (3.3) and (3.4), respectively.

Let $\mu_k = \{\frac{k^2}{l^2}\}_{k\in\mathbb{N}_0}$ be the eigenvalues of $-\triangle$ with homogeneous Neumann boundary condition, $\{\beta_k\}_{k\in\mathbb{N}_0}$ be the corresponding eigenfunctions, then the characteristic equations corresponding to (3.2) are given by

$$\mathcal{P}_k(\lambda, \eta) := Det(\lambda I - D - J) = \lambda^3 + P_k \lambda^2 + Q_k \lambda + R_k(\eta) = 0, \tag{3.7}$$

with

$$\begin{aligned} P_k =& \ (d_N + d_P + d_S)\frac{k^2}{l^2} + \beta - a_{11}, \\ Q_k =& \ (d_N d_p + d_P d_S + d_N d_S)\frac{k^4}{l^4} + [(d_N + d_P)\beta - (d_P + d_S)a_{11} + e\xi N^* P^* g'(N^*)]\frac{k^2}{l^2} \\ &+ eP^* g(N^*) g'(N^*) - \beta a_{11}, \\ R_k(\eta) =& \ d_N d_P d_S \frac{k^6}{l^6} + (d_N d_P \beta - d_P d_S a_{11} + d_S e\xi N^* P^* g'(N^*) + \alpha\xi\eta N^* P^*)\frac{k^4}{l^4} \\ &+ (d_S eP^* g(N^*) g'(N^*) + e\beta\xi N^* P^* g'(N^*) + \alpha\eta P^* g(N^*))\frac{k^2}{l^2} + e\beta P^* g(N^*) g'(N^*). \end{aligned} \tag{3.8}$$

According to (3.7) and (3.8), the eigenvalue problem of (3.6) for $k = 0$ is given by

$$\mathcal{P}_0(\lambda) := (\lambda + \beta)\left(\lambda^2 - a_{11}\lambda + eP^* g(N^*)g'(N^*)\right) = 0,$$

thus we have that when $a_{11} > 0$, $\mathcal{P}_0(\lambda,\eta) = 0$ possesses the eigenvalue with positive real part, when $a_{11} = 0$, $\mathcal{P}_0(\lambda,\eta) = 0$ has a negative root and a pair of purely imaginary roots, then the constant steady state (N^*, P^*, S^*) will be unstable for $a_{11} \geq 0$, then any strategy will be unsuccessful for the system (1.4).

However, when $a_{11} < 0$, the successful measure should be further determined by the specific forms of $f(N)$ and $g(N)$ and the sign of other eigenvalues of (3.7), this is worth discussing in more details. Therefore, in this section, we only consider the situation of $a_{11} < 0$, i.e. $f(N^*) + N^* f'(N^*) - P^* g'(N^*) < 0$. Denote that for $k \in \mathbb{N}_0$,

$$H_1^k = P_k,\quad H_2^k = \begin{pmatrix} P_k & 1 \\ R_k(\eta) & Q_k \end{pmatrix},\quad H_3^k = \begin{pmatrix} P_k & 1 & 0 \\ R_k(\eta) & Q_k & P_k \\ 0 & 0 & R_k(\eta) \end{pmatrix}. \tag{3.9}$$

Next, we present the criteria to determine the stability of E^* by applying to Routh–Hurwitz criterion.

Theorem 3.1. *Suppose that the condition* **(H3)** *holds,* $f(N^*) + N^* f'(N^*) - P^* g'(N^*) < 0$, H_i^k, $i = 1,2,3$, *are defined in* (3.9), *then* $D \vartriangle + J$ *is stable, i.e.* E^* *is stable, if*

$$Det(H_2^k) > 0, \quad \text{for } k \in \mathbb{N},$$

here $Det(H_2^k)$, *denoted as in* (3.10), *represents the determinant of the matrix* H_2^k.

Proof. The assumption **(H3)** assure the unique positive equilibrium E^* exists. By direct calculations, we obtain that

$$\begin{aligned} Det(H_1^k) = &\quad P_k = (d_N + d_P + d_S)\frac{k^2}{l^2} + \beta - a_{11}, \\ Det(H_2^k) = &\quad P_k Q_k - R_k(\eta) = a_1\frac{k^6}{l^6} + a_2\frac{k^4}{l^4} + a_3\frac{k^2}{l^2} + a_4 - \eta\alpha P^*(\xi N^*\frac{k^4}{l^4} + g(N^*)\frac{k^2}{l^2}), \\ Det(H_3^k) = &\quad R_k(\eta)Det(H_2^k) = R_k(\eta)(P_k Q_k - R_k(\eta)), \end{aligned} \tag{3.10}$$

where $k \in \mathbb{N}_0$ and

$$\begin{aligned} a_1 = &\quad (d_N + d_p)(d_N d_p + d_P d_S + d_N d_S) + d_S(d_N d_S + d_P d_S), \\ a_2 = &\quad (d_N^2 + d_P^2 + 2(d_N d_p + d_P d_S + d_N d_S))\beta - (d_P^2 + d_S^2 + 2(d_N d_p + d_P d_S + d_N d_S))a_{11} \\ &\quad + (d_N + d_P)e\xi N^* P^* g'(N^*), \\ a_3 = &\quad (d_P + d_S)a_{11}^2 - 2(d_N + d_P + d_S)\beta a_{11} + (d_N + d_P)(\beta^2 + eP^* g(N^*)g'(N^*)) \\ &\quad - a_{11}\xi e N^* P^* g'(N^*), \\ a_4 = &\quad a_{11}(\beta a_{11} - \beta^2 - eP^* g(N^*)g'(N^*)). \end{aligned} \tag{3.11}$$

In view of (3.8), it follows from $f(N^*) + N^* f'(N^*) - P^* g'(N^*) < 0$, i.e. $a_{11} < 0$ that $P_k > 0$, $Q_k > 0$, $R_k(\eta) > 0$, and $a_1, a_2, a_3, a_4 > 0$ in (3.11). Obviously, $Det(H_1^k) > 0$ for any $k \in \mathbb{N}$, combining with $R_k(\eta) > 0$, we know $Det(H_3^k) > 0$ for any $k \in \mathbb{N}$. Therefore, based on Routh–Hurwitz criterion, all eigenvalues of the matrix $D \vartriangle + J$ have negative real parts if and only of $Det(H_2^k) > 0$ for any $k \in \mathbb{N}$, that means $D \vartriangle + J$ will be stable if $Det(H_2^k) > 0$ for any $k \in \mathbb{N}$. □

According to Theorem 3.1, the key to determine the stability of E^* is to calculate the sign of $Det(H_2^k)$. Taking the derivative of $Det(H_2^k)$ with respect to α, β, ξ, η, then for $k \in \mathbb{N}$, we have

$$\frac{\partial Det(H_2^k)}{\partial \alpha} = -\eta P^*(\xi N^* \frac{k^4}{l^4} + g(N^*)\frac{k^2}{l^2}) < 0, \tag{3.12}$$

$$\frac{\partial Det(H_2^k)}{\partial \eta} = -\alpha P^*(\xi N^* \frac{k^4}{l^4} + g(N^*)\frac{k^2}{l^2}) < 0, \tag{3.13}$$

and for any $\beta > 0$,

$$\begin{aligned} \frac{\partial Det(H_2^k)}{\partial \beta} =& 2\left((d_N + d_P)\frac{k^2}{l^2} - a_{11}\right)\beta + \left(d_N^2 + d_P^2 + 2(d_N d_p + d_P d_S + d_N d_S)\right)\frac{k^4}{l^4} \\ &- 2(d_N + d_P + d_S)a_{11}\frac{k^2}{l^2} + a_{11}^2 > 0, \end{aligned} \tag{3.14}$$

if $(d_N + d_P) \geq \frac{\eta\alpha P^* N^*}{eN^* P^* g'(N^*)}$, then

$$\frac{\partial Det(H_2^k)}{\partial \xi} = \left((d_N + d_P)eN^* P^* g'(N^*) - \eta\alpha P^* N^*\right)\frac{k^4}{l^4} - a_{11}eN^* P^* g'(N^*)\frac{k^2}{l^2} > 0. \tag{3.15}$$

It is worth noting that $\frac{\partial Det(H_2^k)}{\partial \xi} > 0$ for all $k \in \mathbb{N}$ could hold only if $(d_N + d_P) \geq \frac{\eta\alpha P^* N^*}{eN^* P^* g'(N^*)}$ with other parameters being positive and fixed. If $(d_N + d_P) < \frac{\eta\alpha P^* N^*}{eN^* P^* g'(N^*)}$, then there will exist a sufficiently large $k_0 \in \mathbb{N}$ such that $\frac{\partial Det(H_2^k)}{\partial \xi} < 0$, that indicates it is unclear how to determine the dependence of success on the prey-taxis sensitivity when the diffusion rates of prey and predator are small. Consequently, based on Theorem 3.1 and above discussions, we present the following statements:

(i) Decreasing the indirect prey-taxis sensitivity η and the release rate of stimulus α are beneficial measures of success.
(ii) Increasing the decay rate of stimulus β is a beneficial measure of success.
(iii) If the diffusion rates of prey and predator are larger enough, then increasing predator-taxis sensitivity ξ is beneficial to species success.

4. Bifurcation analysis and pattern formation

In terms of the results in Section 3, the weak indirect prey-taxis sensitivity could be beneficial to the stability of system, then a natural question raises that whether the strong indirect prey-taxis sensitivity will promote the emergence of patterns? In this section we will choose the rate of indirect prey-taxis coefficient η being a bifurcation parameter to study the existence of bifurcations for the system (1.4), including Hopf and double-Hopf bifurcations, and also determine the stability of the positive constant steady state.

A k-mode Hopf bifurcation occurs if the characteristic equation $\mathcal{P}_k(\lambda) = 0$ has a pair of purely imaginary eigenvalues, all other roots of $\mathcal{P}_j(\lambda) = 0$, for $j \in \mathbb{N}_0$ and $j \neq k$, have nonzero real parts, and the corresponding transversality condition is satisfied. As in [46], we say that system undergoes (k_1, k_2)-mode double-Hopf bifurcation if all roots of $\mathcal{P}_k(\lambda) = 0$, for $k \in \mathbb{N}_0$ and $k \neq k_1, k_2$, have nonzero real parts, except a pair of purely imaginary eigenvalues for $\mathcal{P}_{k_i}(\lambda) = 0$, $k_i \in \mathbb{N}_0, i = 1, 2$, and the respective transversality conditions are satisfied. Similarly, (k_1, k_2, k_3)-mode triple-Hopf bifurcation can be defined as well for $k_i \in \mathbb{N}_0, i = 1, 2, 3$.

As illustrated in Section 3, when $f(N^*) + N^* f'(N^*) - P^* g'(N^*) = 0$, the characteristic Eqs. (3.7) have a pair of purely imaginary eigenvalues at least, this indicates 0-mode Hopf bifurcation may occur. To completely analyze the bifurcations distribution of (1.4), so to this end, we posit the following hypothesis:

(H4) $f(N^*) + N^* f'(N^*) - P^* g'(N^*) \leq 0$.

Remark 4.1. The expression of (3.8) shows $R_k(\eta) > 0$ for any $a_{11} \leq 0$, then there is no simple zero eigenvalue for the characteristic Eqs. (3.7), which means that if the assumption **(H4)** is satisfied, Turing bifurcation is impossible for the system (1.4).

If (3.7) possesses a pair of purely imaginary eigenvalues $\pm i\omega_k$, then plugging $\lambda = i\omega_k$ into (3.7), we gain the existence condition of Hopf bifurcation

$$P_k Q_k - R_k(\eta) = 0, \tag{4.1}$$

to discuss the effect of indirect prey-taxis sensitivity on the dynamics of (1.4), we can establish the existence conditions of Hopf bifurcations: For $k \in \mathbb{N}$,

$$\eta = \eta_k^H := \frac{a_1 \frac{k^6}{l^6} + a_2 \frac{k^4}{l^4} + a_3 \frac{k^2}{l^2} + a_4}{\alpha P^* (\xi N^* \frac{k^4}{l^4} + g(N^*) \frac{k^2}{l^2})} > 0, \tag{4.2}$$

where a_1, a_2, a_3, a_4 are given by (3.11). For $k = 0$,

$$f(N^*) + N^* f'(N^*) - P^* g'(N^*) = 0,$$

and

$$\omega_0 = \sqrt{e P^* g(N^*) g'(N^*)}, \qquad \omega_k = \sqrt{Q_k}, \text{ for } k \in \mathbb{N}, \tag{4.3}$$

where $Q_k(\eta_k^H) > 0$. Subsequently, we verify transversality conditions as follows:

Remark 4.2. Via differentiating Eq. (3.7) with respect to η at $\eta = \eta_k^H$, we derive that

$$Re\left(\frac{d\lambda}{d\eta}\right)^{-1}\Bigg|_{\eta=\eta_k^H} = -\frac{3\lambda^2 + 2P_k\lambda + Q_k}{\alpha P^* (\xi N^* \frac{k^4}{l^4} + g(N^*) \frac{k^2}{l^2})} = \frac{2Q_k}{\alpha P^* (\xi N^* \frac{k^4}{l^4} + g(N^*) \frac{k^2}{l^2})} > 0. \tag{4.4}$$

Since the sign of $\frac{dRe\lambda}{d\eta}$ is equivalent to the sign of $Re\left(\frac{d\lambda}{d\eta}\right)^{-1}$, hence $\frac{dRe\lambda}{d\eta}\Big|_{\eta=\eta_k^H} > 0$.

Next we can state the results on Hopf bifurcations of (1.4).

Proposition 4.3. *For $d_N, d_P, d_S, e, m, \alpha, \beta, \xi > 0$, suppose that the condition **(H3)-(H4)** hold, a_{11}, η_k^H are defined as in (3.5) and (4.2).*

(i) *If $a_{11} < 0$, $\eta_j^H \neq \eta_k^H$ for any $k, j \in \mathbb{N}, j \neq k$, then the system (1.4) undergoes k-mode Hopf bifurcation near the positive constant steady state E^* at $\eta = \eta_k^H, k \in \mathbb{N}$, the bifurcating periodic solution is spatially nonhomogeneous.*
(ii) *If $a_{11} = 0$, then the system (1.4) undergoes 0-mode Hopf bifurcation near the positive constant steady state E^*, provided by $\eta \neq \eta_k^H, k \in \mathbb{N}$, the bifurcating periodic solution is spatially homogeneous.*

Proof. Via (3.10), we can derive the existence conditions of Hopf bifurcations by two situations, i.e. for $k \in \mathbb{N}$,

$$\eta = \eta_k^H,$$

here η_k^H is defined in (4.2). For $k=0$,

$$f(N^*)+N^*f'(N^*)-P^*g'(N^*)=0,$$

Then the rest proof is divided into two parts.

For the part (i), if $f(N^*)+N^*f'(N^*)-P^*g'(N^*)<0$, i.e. $a_{11}<0$, we have that

$$\mathcal{P}_0(\lambda):=(\lambda+\beta)\left(\lambda^2-a_{11}\lambda+eP^*g(N^*)g'(N^*)\right)=0,$$

then the characteristic equation $\mathcal{P}_0(\lambda)=0$ has negative real eigenvalues. When $\eta=\eta_k^H$ and $\eta_j^H\neq\eta_k^H$ for any $k,j\in\mathbb{N},j\neq k$, since $\eta=\eta_k^H$ is the unique positive solution of (4.1), it is easy to know that the characteristic equation for each $k\in\mathbb{N}$ has a pair of purely imaginary eigenvalues, and other characteristic equations have eigenvalues with nonzero real parts, and transversality condition holds as in Remark 4.2. Therefore the system (1.4) undergoes k-mode Hopf bifurcation near the positive constant steady state E^*.

For the part (ii), if $f(N^*)+N^*f'(N^*)-P^*g'(N^*)=0$, i.e. $a_{11}=0$, then the characteristic equation $\mathcal{P}_0(\lambda)=0$ has a pair of purely imaginary eigenvalues. When $\eta\neq\eta_k^H,k\in\mathbb{N}$, there are no eigenvalues with zero real parts for all $\mathcal{P}_k(\lambda,\eta)=0,k\in\mathbb{N}$, thus the system (1.4) undergoes 0-mode Hopf bifurcation near the positive constant steady state E^*. □

Theorem 4.4. *For $d_N,d_P,d_S,e,m,\alpha,\beta,\xi>0$, a_{11}, $\eta_k^H,k\in\mathbb{N}$ are defined as in (3.5) and (4.2), suppose that the condition **(H3)-(H4)** hold, and $a_{11}<0$. If there exist $k_i,i\in\mathbb{N},i\leq 4$, such that $\eta_{k_1}^H=\cdots=\eta_{k_i}^H$, then the system (1.4) undergoes i-multiple Hopf bifurcation near the positive constant steady state E^*. In particular, if $i\leq 2$, then (k_1,k_2)-mode double-Hopf bifurcation. Moreover, the positive constant steady state E^* is locally asymptotically stable for $\eta<\min_{k\in\mathbb{N}}\eta_k^H$ and unstable for $\eta>\min_{k\in\mathbb{N}}\eta_k^H$.*

Proof. According to (4.2), denote

$$r:=\alpha\xi N^*P^*,\quad q:=\alpha P^*g(N^*), \tag{4.5}$$

and

$$G_1(x):=\frac{a_1x^3+a_2x^2+a_3x+a_4}{rx^2+qx},\quad \text{for } x>0, \tag{4.6}$$

with a_1,a_2,a_3,a_4 are given in (3.11). By direct calculating, we obtain

$$G_1'(x)=\tfrac{1}{(rx^2+qx)^2}\left(a_1rx^4+2a_1qx^3+(a_2q-a_3r)x^2-a_4q\right),\quad \text{for } x>0. \tag{4.7}$$

It is obvious that the sign of $G_1'(x)$ is equivalent to the sign of the following function

$$h(x):=a_1rx^4+2a_1qx^3+(a_2q-a_3r)x^2-a_4q, \tag{4.8}$$

here $a_1,a_2,a_3,a_4,r,q>0$. Since $h(x)=0$ has at most four roots, $h(0)<0$, $\lim_{x\to-\infty}h(x)=+\infty$, $\lim_{x\to+\infty}h(x)=+\infty$ imply that there exists at least one solution of $h(x)=0$ for $x\in(0,+\infty)$. Hence the possible real root distribution of $h(x)=0$ may be divided into three cases:

(a) there exists only a simple real root of $h(x)=0$ for $x\in(0,+\infty)$;
(b) there exist a simple real root and a real double root of $h(x)=0$ for $x\in(0,+\infty)$;
(c) there exist three different real root of $h(x)=0$ for $x\in(0,+\infty)$. □

For case (a) and (b), there will exist a $x_1>0$ such that $G_1(x)$ is decreasing for $x\in(0,x_1)$ and increasing for $x\in(x_1,+\infty)$, so in these cases, there can only be at most two different $k_i\in\mathbb{N},i=1,2$, such that $\eta_{k_1}=\eta_{k_2}$. For the case (c), there will exist $x_1,x_2,x_3>0$ such that $G_1(x)$ is decreasing for $x\in(0,x_1)\cup(x_2,x_3)$ and increasing for $x\in(x_1,x_2)\cup(x_3,+\infty)$, similarly, in these cases, there may be at most four different $k_i,i\in\mathbb{N},i\leq 4$, such that $\eta_{k_1}^H=\cdots=\eta_{k_i}^H$.

In addition, based on the above monotonicity of $G(x)$, we conclude that the minimum of η_k^H is reachable, denoted by $\min_{k\in\mathbb{N}}\eta_k^H$, so the positive equilibrium is locally asymptotically stable for $\eta<\min_{k\in\mathbb{N}}\eta_k^H$ and unstable for $\eta>\min_{k\in\mathbb{N}}\eta_k^H$.

Moreover, if there exist some $k_i\in\mathbb{N}$, such that $\eta_{k_1}^H=\cdots=\eta_{k_i}^H$, then when $\eta=\eta_{k_i}^H$, the characteristic $\mathcal{P}_{k_i}(\eta)$ will possess a pair of purely imaginary eigenvalues for such $k_i\in\mathbb{N}$, this indicates the system will have i pairs of purely imaginary eigenvalues, and other eigenvalues have nonzero real parts, Remark 4.2 guarantees that corresponding transversality condition holds. Therefore, the system (1.4) undergoes i-multiple Hopf bifurcation near the positive constant steady state E^* at $\eta=\eta_{k_i}^H$.

If $a_{11}=0$, it is easy to know $a_4=0$. Review the expression (4.2) and (4.5), we denote

$$G_2(x):=\frac{a_1x^2+a_2x+a_3}{rx+q},\quad \text{for } x>0. \tag{4.9}$$

To further establish the existence conditions of double-Hopf bifurcations for $f(N^*)+N^*f'(N^*)-P^*g'(N^*)=0$ and determine the stability of the positive equilibrium, we first give the following results.

Lemma 4.5. *For $d_N,d_P,d_S,e,m,\alpha,\beta$, a_{11}, $\eta_k^H,k\in\mathbb{N}$ are defined as in (3.5) and (4.2), suppose $a_{11}=0$, define*

$$\xi^*=\frac{(d_N^2+d_P^2+2(d_Nd_P+d_Nd_S+d_Pd_S))g(N^*)}{(d_N+d_P)\beta N^*}. \tag{4.10}$$

(i) *If* $\xi \le \xi^*$, *then* $\eta_1^H = \min_{k\in\mathbb{N}} \eta_k^H$.
(ii) *If* $\xi > \xi^*$, *then there exists* $k^* \in \mathbb{N}$ *such that* $\eta_{k^*}^H = \min_{k\in\mathbb{N}} \eta_k^H$, *where*

$$k^* = \begin{cases} \lfloor l\sqrt{x^*}\rfloor, & \text{for } \eta^H_{\lfloor l\sqrt{x^*}\rfloor} \le \eta^H_{\lfloor l\sqrt{x^*}\rfloor+1}, \\ \lfloor l\sqrt{x^*}\rfloor + 1, & \text{for } \eta^H_{\lfloor l\sqrt{x^*}\rfloor} > \eta^H_{\lfloor l\sqrt{x^*}\rfloor+1}, \end{cases} \tag{4.11}$$

with x^* *is the unique positive root of* $x^2 + \frac{2q}{r}x + \frac{a_2 q - a_3 r}{r} = 0$. a_2, a_3 *are defined as in* (3.11). *In particular, it is asserted* $k^* = 1$ *when* $l\sqrt{x^*} < 1$.

Proof. Similar to the proof of Theorem 4.4, we can compute the derivative of $G_2(x)$,

$$G_2'(x) = \frac{1}{(rx+q)^2}\left(a_1 r x^2 + 2a_1 q x + (a_2 q - a_3 r)\right), \quad \text{for } x > 0.$$

By the views of a_2, a_3 in (3.11) and (4.5), when $\xi \le \xi^*$, $a_2 q - a_3 r \ge 0$, then $G_2'(x) > 0$ for any $x \in (0, +\infty)$, then $G_2(x)$ is increasing for $x \in (0, +\infty)$, which means η_k^H is increasing in $k \in \mathbb{N}$, thus $\eta_1^H = \min_{k\in\mathbb{N}} \eta_k^H$.

When $\xi > \xi^*$, $a_2 q - a_3 r < 0$, then there exists a $x^* \in (0, +\infty)$ such that $G_2'(x) = 0$. So $G_2(x)$ is decreasing for $x \in (0, x^*)$ and increasing for $x \in (x^*, +\infty)$, which implies that η_k^H can attain the minimum at k^* with k^* defined as in (4.11). In addition, when $l\sqrt{x^*} < 1$, we assert $k^* = 1$. □

Combine the similar argument as the proof of Theorem 4.4 and Lemma 4.5, we derive the existence of double-Hopf bifurcation and the stability of the positive equilibrium for $f(N^*) + N^* f'(N^*) - P^* g'(N^*) = 0$, stated as in the following theorem.

Theorem 4.6. *For* $d_N, d_P, d_S, e, m, \alpha, \beta > 0$, a_{11}, η_k^H, ξ^*, k^* *are defined as in* (3.5), (4.2), (4.10) *and* (4.11). *Suppose the conditions **(H3)-(H4)** hold, If* $a_{11} = 0$, $\eta = \eta_k^H$ *and* $\eta_j^H \ne \eta_k^H$ *for any* $k, j \in \mathbb{N}, j \ne k$, *then the system* (1.4) *undergoes* $(k, 0)$*-mode double-Hopf bifurcation near* E^*. *Moreover, the following statements hold:*

(i) *When* $\xi \le \xi^*$, *the positive constant steady state* E^* *destabilizes through* $(1, 0)$*-mode double-Hopf bifurcation.*
(ii) *When* $\xi > \xi^*$, *the positive constant steady state* E^* *destabilizes through* $(k^*, 0)$*-mode double-Hopf bifurcation, provided by* $\eta_{k^*}^H \ne \eta_{k^*+1}^H$,

$$\eta_{k^*}^H = \frac{a_1 \frac{k^{*4}}{l^4} + a_2 \frac{k^{*2}}{l^2} + a_3}{\alpha P^*(\xi N^* \frac{k^{*2}}{l^2} + g(N^*))}, \tag{4.12}$$

where a_1, a_2, a_3 *are defined as in* (3.11) *satisfying* $k = k^*$.

Otherwise, the positive constant steady state E^* *loses the stability through* 0*-mode Hopf bifurcation.*

Remark 4.7. $a_{11} = 0$, i.e. $f(N^*) + N^* f'(N^*) - P^* g'(N^*) = 0$ is the existence condition of Hopf bifurcation for $k = 0$, Under this condition, if additionally consider the prey-taxis sensitivity coefficient η as a bifurcation parameter, then $(k, 0)$-mode double-Hopf bifurcations near the positive equilibrium for any $k \in \mathbb{N}$. In particular, as mentioned in Theorem 4.6, $(1, 0)$ and $(k^*, 0)$-mode double-Hopf bifurcations are the corresponding first double-Hopf bifurcation which destablizes the positive equilibrium in some appropriate conditions.

5. Application to Rosenzweig–MacArthur model with indirect prey-taxis and direct predator-taxis

5.1. Local stability and double-Hopf bifurcation

This subsection is devoted to applying the results derived in Section 2 to a classical diffusive Rosenzweig–MacArthur model. A new finding is that the large indirect prey-taxis rate can induce the occurrence of spatially nonhomogeneous Hopf and double-Hopf bifurcations, this will lead to complex spatiotemporal patterns emerging.

Corresponding to (1.4), by setting

$$f(N) = 1 - \frac{N}{K}, \quad g(N) = \frac{\gamma N}{1+N}, \quad e = 1, \tag{5.1}$$

we derive the following predator–prey model with prey-taxis and predator-taxis:

$$\begin{cases} N_t = d_N \triangle N + \xi\nabla\cdot(N\nabla P) + N\left(1 - \frac{N}{K}\right) - \frac{\gamma N P}{1+N}, & x \in (0, l\pi),\ t > 0, \\ P_t = d_P \triangle P - \eta\nabla\cdot(P\nabla S) + \frac{\gamma N P}{1+N} - mP, & x \in (0, l\pi),\ t > 0, \\ S_t = d_S \triangle S + \alpha N - \beta S, & x \in (0, l\pi),\ t > 0, \\ \frac{\partial N}{\partial \nu} = \frac{\partial N}{\partial \nu} = \frac{\partial N}{\partial \nu} = 0, & x = 0, l\pi, t > 0, \\ N(x,0) = N_0(x) > 0, \quad P(x,0) = P_0(x) > 0, \quad S(x,0) = S_0(x) > 0, & x \in (0, l\pi). \end{cases} \tag{5.2}$$

Assume that

$$\gamma > \frac{m(1+K)}{K},$$

then the system (5.2) has a unique positive equilibrium, denoted by $E^* = (N^*, P^*, S^*)$ with

$$N^* = \frac{m}{\gamma - m}, \quad P^* = \frac{(K-N^*)(1+N^*)}{\gamma K}, \quad S^* = \frac{\alpha m}{\beta(\gamma - m)}.$$

Linearize the system (5.2) at the positive equilibrium E^*, we derive

$$\begin{cases} N_t = d_N \triangle N + \xi N^* \triangle P + \dfrac{N^*(K-2N^*-1)}{K(1+N^*)} N - \dfrac{\gamma N^*}{1+N^*} P, \\ P_t = d_P \triangle P - \frac{\eta(K-N^*)(1+N^*)}{K\gamma} \triangle S + \dfrac{K-N^*}{K(1+N^*)} N, \\ S_t = d_S \triangle S + \alpha N - \beta S, \end{cases} \tag{5.3}$$

as in (3.3) and (3.4), we denote that

$$D = \begin{pmatrix} d_N & \xi N^* & 0 \\ 0 & d_P & -\frac{\eta(K-N^*)(1+N^*)}{K\gamma} \\ 0 & 0 & d_S \end{pmatrix}, \tag{5.4}$$

$$J = \begin{pmatrix} \frac{N^*(K-2N^*-1)}{K(1+N^*)} & m & 0 \\ -\frac{(K-N^*)}{K(1+N^*)} & 0 & 0 \\ \alpha & 0 & -\beta \end{pmatrix}. \tag{5.5}$$

Denote that

$$a_{11} = \frac{N^*(K-2N^*-1)}{K(1+N^*)}, \tag{5.6}$$

we also have

$$\eta_k^H = \frac{a_1 \frac{k^6}{l^6} + a_2 \frac{k^4}{l^4} + a_3 \frac{k^2}{l^2} + a_4}{\alpha N^* P^* \frac{k^2}{l^2}(\xi \frac{k^2}{l^2} + \frac{\gamma}{1+N^*})}, \quad k \in \mathbb{N}, \tag{5.7}$$

here a_1, a_2, a_3, a_4 satisfy (3.11) and (5.1). Then based on the analyses in Section 4, we present the following conclusions for the dynamics of (5.2).

Proposition 5.1. *Suppose that η_k^H are given in (5.7), then the following statements hold:*

(i) *If $K \le 1$ or $K > 1$, $\frac{m(K+1)}{K} < \gamma < \frac{m(K+1)}{K-1}$, then the system (5.2) undergoes k-mode Hopf bifurcation near the positive constant steady state E^* at $\eta = \eta_k^H$, $k \in \mathbb{N}$, and bifurcating periodic solution is spatially nonhomogeneous.*

(ii) *If $K > 1$, $\gamma = \frac{m(K+1)}{K-1}$, then the system (5.2) undergoes 0-mode Hopf bifurcation near the positive constant steady state E^*, provided by $\eta \ne \eta_k^H(\frac{m(K+1)}{K-1})$, $k \in \mathbb{N}$, and bifurcating periodic solution is spatially homogeneous.*

Proof. Choose γ being a bifurcation parameter, then when $K \le 1$, $a_{11} < 0$ is always true. when $K > 1$,

$$a_{11} \begin{cases} < 0, & \text{for } \gamma < \frac{m(K+1)}{K-1}, \\ = 0, & \text{for } \gamma = \frac{m(K+1)}{K-1}, \\ > 0, & \text{for } \gamma > \frac{m(K+1)}{K-1}. \end{cases}$$

Combining the basic assumption $\frac{m(K+1)}{K} < \gamma$ and Proposition 4.3-(i), the part (i) is proved.

When $K > 1$ and $\gamma = \frac{m(K+1)}{K-1}$

$$\mathcal{P}_0(\lambda) := \lambda^3 + (\beta - a_{11})\lambda^2 + \left(\frac{\gamma N^*(K-N^*)^*}{K(1+N^*)} - \beta a_{11}\right)\lambda + \frac{\beta\gamma N^*(K-N^*)}{K(1+N^*)^*} = 0,$$

we can calculate the transversality condition by taking the derivative of $\mathcal{P}_0(\lambda) = 0$ as follows

$$\left(3\lambda^3 + 2(\beta - a_{11})\lambda + \frac{\gamma N^*(K-N^*)}{K(1+N^*)^*} - (\beta a_{11})\right) \frac{d\lambda}{d\gamma}\bigg|_{\gamma = \frac{m(K+1)}{K-1}} = -\beta \frac{d}{d\gamma}\left(\frac{\gamma N^*(K-N^*)}{K(1+N^*)^*}\right)\bigg|_{\gamma = \frac{m(K+1)}{K-1}},$$

then

$$Re\left(\frac{d\lambda}{d\gamma}\right)^{-1}\bigg|_{\gamma = \frac{m(K+1)}{K-1}} = \frac{2\gamma N^*(K-N^*)}{\beta K(1+N^*)^*} \frac{d}{d\gamma}\left(\frac{\gamma N^*(K-N^*)}{K(1+N^*)^*}\right)\bigg|_{\gamma = \frac{m(K+1)}{K-1}},$$

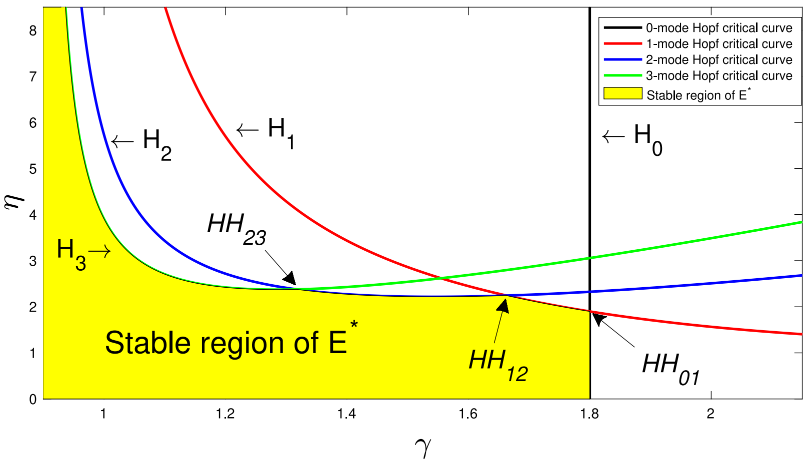

(a) $\xi = 1.5$, $k^* = 1$.

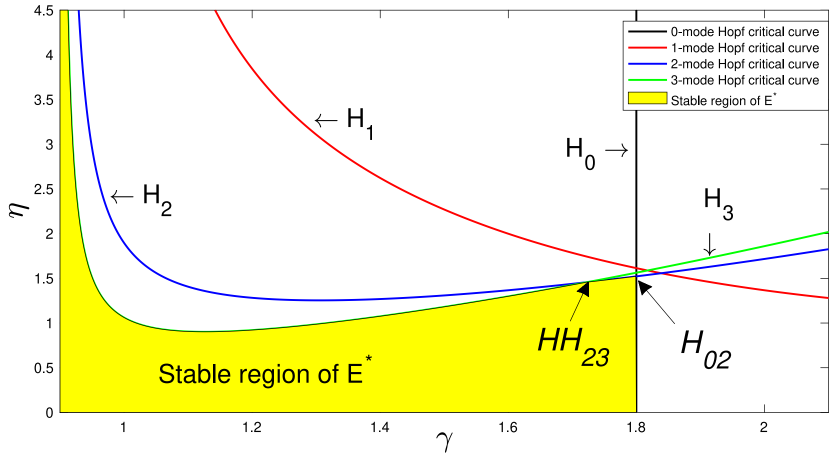

(b) For $\xi = 10.5$, $k^* = 2$.

Fig. 1. For fixed parameters $d_N = 0.4, d_P = 0.8, d_S = 0.4, \alpha = 1, \beta = 0.5, m = 0.6, K = 2, l = 4$, $\xi^* = 4.8$, corresponding bifurcation graphs for $\xi \le \xi^*$ and $\xi > \xi^*$. Here $H_i, i = 0, 1, 2, 3$ represent Hopf critical curves, H_{01}, H_{02}, H_{12}, H_{23} match with $(0,1)$, $(0,2)$, $(1,2)$, $(2,3)$-mode double-Hopf bifurcation points, respectively.

which means that the sign of $\frac{dRe\lambda}{d\gamma}$ is same as $\frac{d}{d\gamma}\left(\frac{\gamma N^*(K-N^*)}{K(1+N^*)^*}\right)$, and

$$\frac{d}{d\gamma}\left(\frac{\gamma N^*(K-N^*)}{K(1+N^*)^*}\right)\Bigg|_{\gamma=\frac{m(K+1)}{K-1}} = m > 0,$$

then the transversality condition holds. Therefore, by Proposition 4.3-(ii), the part (ii) is proved. □

Next following Theorems 4.4, 4.6 and Proposition 5.1, we establish the existence conditions of double-Hopf bifurcations and the stability of the positive constant steady state is further determined.

Proposition 5.2. *Suppose that $K \le 1$ or $K > 1$, $\frac{m(K+1)}{K} < \gamma < \frac{m(K+1)}{K-1}$, η_k^H, $k \in \mathbb{N}$ are given in (5.7). If there exist $i, j \in \mathbb{N}$, $i \ne j$, such that $\eta_i^H = \eta_j^H$, then the system (5.2) undergoes (i,j)-mode double-Hopf bifurcation, provided by $\eta_k^H \ne \eta_i^H$ for any $k \in \mathbb{N}, k \ne i, j$. Moreover, the constant steady state E^* of system (1.4) is locally asymptotically stable for $\eta < \min_{k\in\mathbb{N}} \eta_k^H$ and unstable for $\eta > \min_{k\in\mathbb{N}} \eta_k^H$.*

Proposition 5.3. *Suppose that $\gamma = \frac{m(K+1)}{K-1}$ for $K > 1$, ξ^*, $\eta_k^H, k \in \mathbb{N}$ are given in (4.10), (5.7), If $\eta = \eta_k^H$ and $\eta_j^H \ne \eta_k^H$ for any $k, j \in \mathbb{N}, j \ne k$, then the system (1.4) undergoes $(k,0)$-mode double-Hopf bifurcation near E^*. Moreover, the following statements hold:*

(i) *When $\xi \le \xi^*$, the positive constant steady state E^* destabilizes through $(1,0)$-mode double-Hopf bifurcation.*

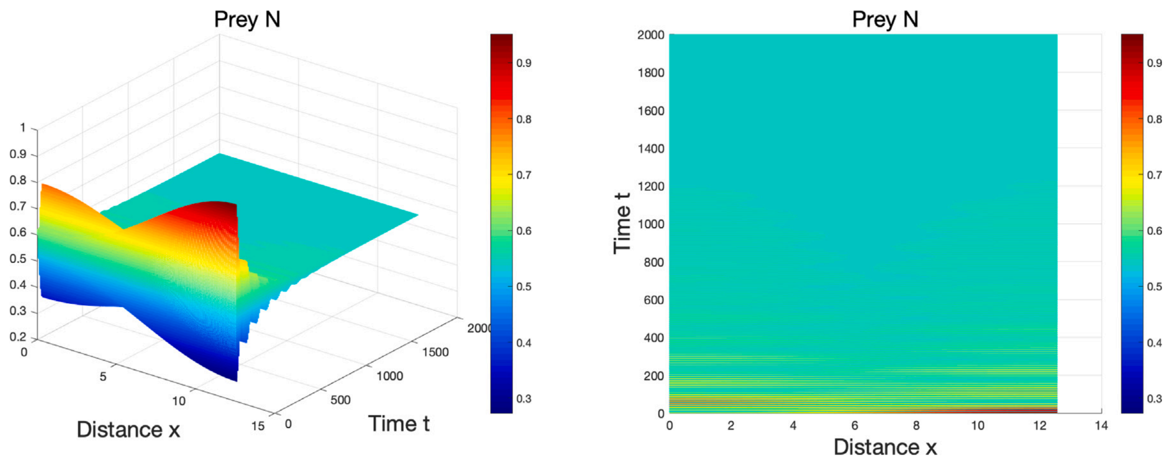

Fig. 2. For parameters $\gamma = 1.6, \eta = 1.5987$, initial conditions $N(x,0) = P(x,0) = S(x,0) = 0.5 + 0.1\cos(\frac{x}{4})$, the coexistence steady state $E^* \approx (0.6, 0.7, 1.2)$ of (1.4). The right graph shows corresponding projections of $N(x,t)$ on (x,t)-plane. Graphs of P, S are similar to N, we omit here.

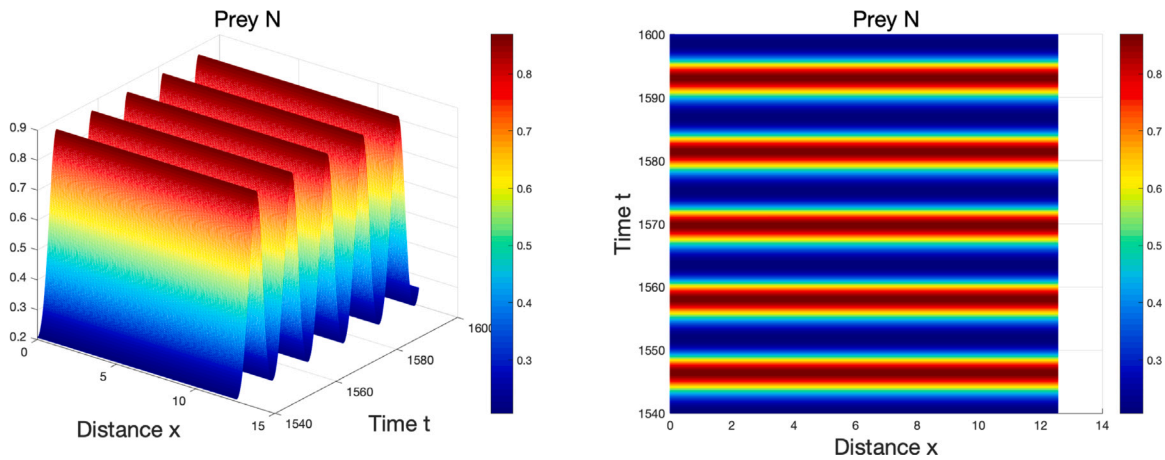

Fig. 3. For parameters $\gamma = 1.9, \eta = 1.5987$, initial conditions $N(x,0) = P(x,0) = S(x,0) = 0.5 + 0.3\cos(\frac{x}{4})$, spatially homogeneous periodic solution of (1.4) and corresponding projections of $N(x,t)$ on (x,t)-plane. Graphs of P, S are similar to N, we omit here.

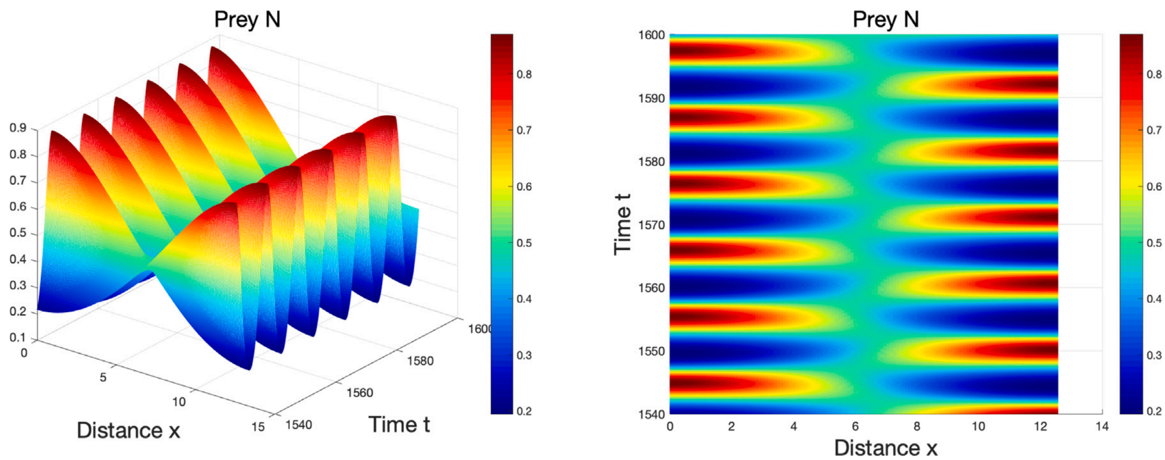

Fig. 4. For parameters $\gamma = 1.9, \eta = 1.9987$, initial conditions $N(x,0) = P(x,0) = S(x,0) = 0.5 + 0.3\cos(\frac{x}{4})$, spatially nonhomogeneous periodic solution with one spatial frequency of (1.4), and corresponding projections of $N(x,t)$ on (x,t)-plane. Graphs of P, S are similar to N, we omit here.

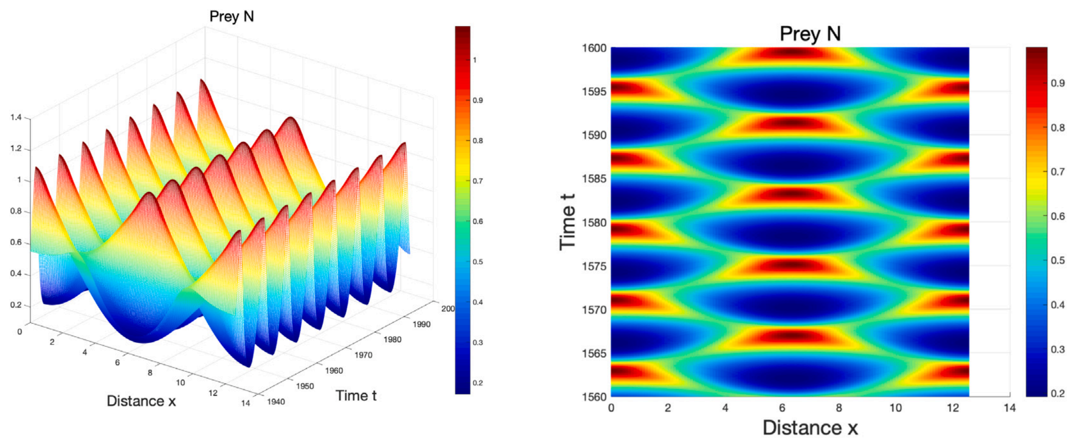

(a)

Fig. 5. For parameters $\gamma = 1.9, \eta = 2.5987$, initial conditions $N(x,0) = P(x,0) = S(x,0) = 0.5 + 0.3\cos(\frac{x}{2})$, spatially nonhomogeneous periodic solutions with two spatial frequencies of (1.4) and corresponding projections of $N(x,t)$ on (x,t)-plane. Graphs of P, S are similar to N, we omit here.

(ii) *When $\xi > \xi^*$, the positive constant steady state E^* destabilizes through $(k^*, 0)$-mode double-Hopf bifurcation, provided by $\eta^H_{k^*} \neq \eta^H_{k^*+1}$,*

$$\eta^H_{k^*} = \frac{a_1 \frac{k^{*4}}{l^4} + a_2 \frac{k^{*2}}{l^2} + a_3}{\alpha N^* P^* (\xi \frac{k^{*2}}{l^2} + \frac{\gamma}{1+N^*})}, \tag{5.8}$$

where

$$\begin{aligned} a_1 &= (d_N + d_P)(d_N d_P + d_P d_S + d_N d_S) + d_S(d_N d_S + d_P d_S), \\ a_2 &= (d_N^2 + d_P^2 + 2(d_N d_P + d_P d_S + d_N d_S))\beta + \frac{(d_N + d_P)\gamma \xi N^* P^*}{(1+N^*)^2}, \\ a_3 &= (d_N + d_P)\left(\beta^2 + \frac{\gamma^2 N^* P^*}{(1+N^*)^3}\right). \end{aligned} \tag{5.9}$$

Otherwise, the positive constant steady state E^* loses the stability through 0-mode Hopf bifurcation.

Corollary 5.4. *Suppose that ξ^*, η^H_k for $k \in \mathbb{N}$ are given in (4.10), (5.7), then the following statements hold:*

(i) *If $K \le 1$ or $K > 1$, $\frac{m(K+1)}{K} < \gamma < \frac{m(K+1)}{K-1}$; then the positive constant steady state E^* is locally asymptotically stable for $\eta < \min_{k\in\mathbb{N}} \eta^H_k$ and unstable for $\eta > \min_{k\in\mathbb{N}} \eta^H_k$.*
(ii) *If $\gamma = \frac{m(K+1)}{K-1}$ for $K > 1$, then the positive constant steady state E^* is unstable for any $\eta > 0$.*

5.2. Pattern formation

In this section, some numerical simulations are performed to support the previous theoretical results. We fix parameter values as follow:

$$m = 0.6,\ K = 2,\ \alpha = 1,\ \beta = 0.5,\ l = 4, \tag{5.10}$$

and

$$d_N = 0.4,\ d_P = 0.8,\ d_S = 0.4, \tag{5.11}$$

then we can derive that $\gamma^* = 1.8$, when $\gamma = \gamma^*$, we have

$$f(N^*) + N^* f'(N^*) - P^* g'(N^*) = 0,$$

that implies the system (1.4) will undergoes a 0-mode Hopf bifurcation and a spatially homogeneous periodic solution arises. Further, we can determine that $\xi^* = 4.8$ defined in (4.10), then following Lemma 4.5, we have that

$$\min_{k\in\mathbb{N}} \eta^H_k = \begin{cases} \eta^H_1, & \text{for } \xi \le \xi^*, \\ \eta^H_{k^*}, & \text{for } \xi > \xi^*, \end{cases} \tag{5.12}$$

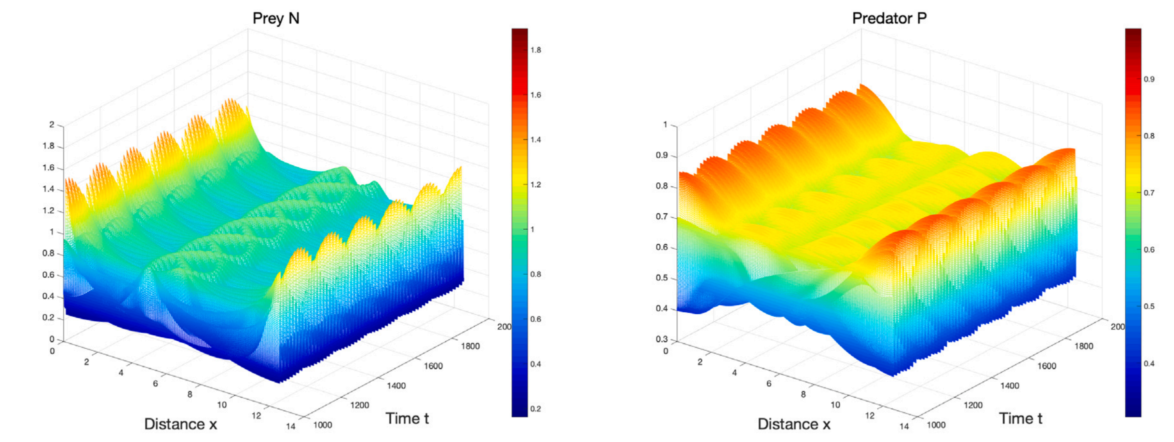

(a)

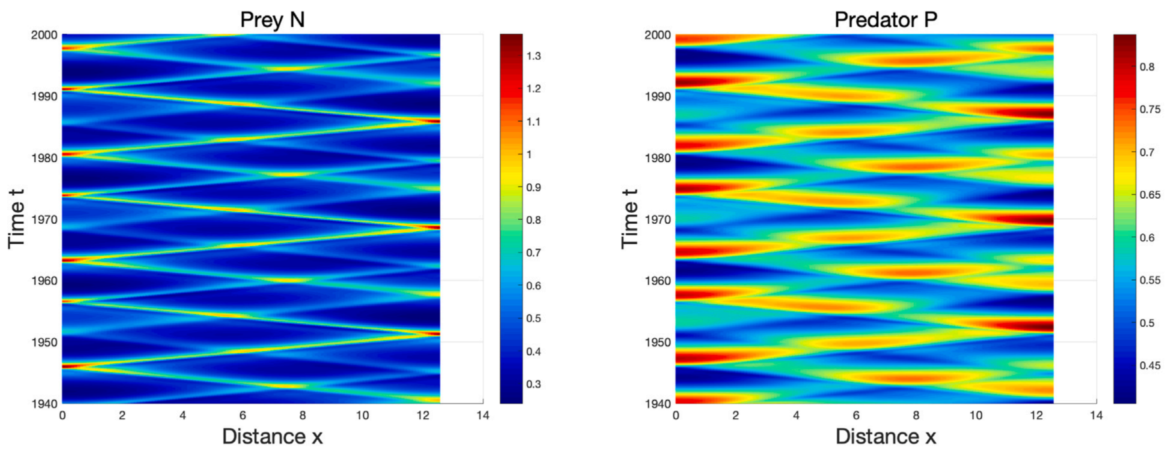

(b) The projections of graphs in (a) on (x, t)-plane

Fig. 6. For parameters $\gamma = 1.9, \eta = 1.6222$, initial conditions $N(x,0) = P(x,0) = S(x,0) = 0.5 + 0.1\cos(\frac{x}{4})$, Spatially nonhomogeneous quasi-periodic solutions of (1.4) and corresponding spatiotemporal patterns. The graph of S is similar, we omit here.

where k^* defined as in (4.11), and it can be calculated that $\eta_1^H \approx 1.8987$ for $\xi = 1.5$, Fig. 1-(a) exhibits concrete bifurcation graph. For the case of $\xi > 4.8$, for example, we choose $\xi = 10.5$ here, one can find that $k^* = 2$ and $\eta_2^H \approx 1.5222$, corresponding bifurcation is shown as in Fig. 1-(b). It is worth noting that the bifurcation graph for the situation in Proposition 5.2, i.e. $a_{11} < 0$, is analogous except that there is no H_0 in the graph, so we do not plot this case.

It follows Theorem 4.6 that we have the following statement for the dynamics of (5.2) under the given parameter conditions.

Proposition 5.5. *If $m = 0.6$, $K = 2$, $l = 4, \alpha = 1$, $\beta = 0.5$, $d_N = 0.4$, $d_P = 0.8$, $d_S = 0.4$, and $\gamma = \gamma^* = 1.8$, then*

(i) *when $\xi \le 4.8$, the positive constant steady state E^* of (5.2) is destabilized through $(1,0)$-mode double-Hopf bifurcation near E^* at $(\gamma, \eta) = (\gamma^*, \eta_1^H) = (1.8, 1.8987)$.*

(ii) *when $\xi > 4.8$, e.g. $\xi = 10.5$, the positive constant steady state E^* of (5.2) is destabilized through $(2,0)$-mode double-Hopf bifurcation near E^* at $(\gamma, \eta) = (\gamma^*, \eta_2^H) = (1.8, 1.5222)$.*

It is well known that Hopf bifurcation can be used to theoretically prove the existence of periodic solutions, and quasi-periodic or multi-periodic solutions even chaos can be found near the double-Hopf singularity. Consequently, we will present some numerical simulations to state the spatiotemporal dynamics of (5.2) based on Proposition 5.5.

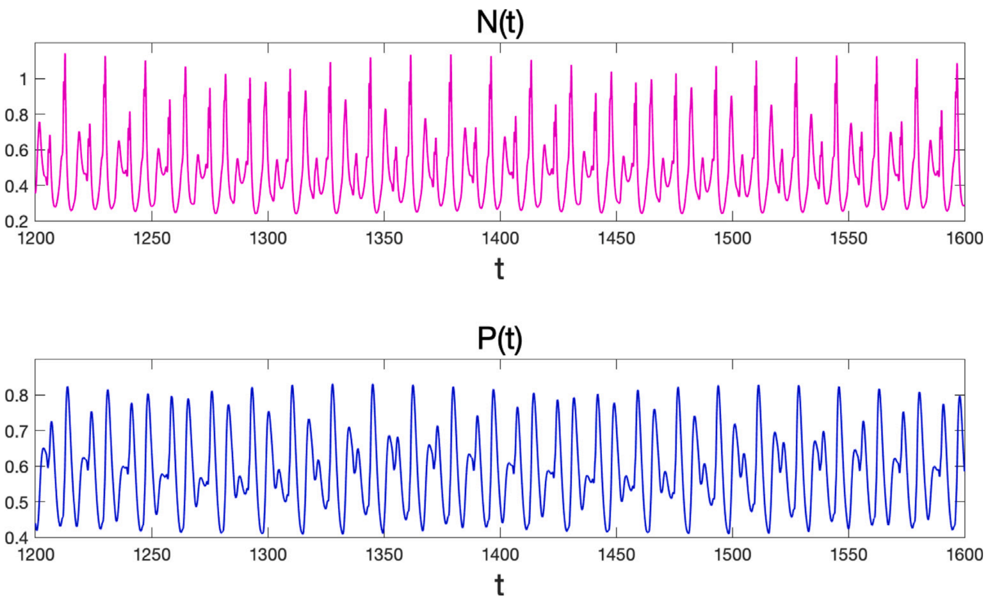

Fig. 7. Graphs of quasi-periodic solution in Fig. 6 for a fixed space location $x = 8$.

For Fig. 2, since the shape of S completely follows the shape of N and P, thus for the sake of simplification, we omit the graph of S. Figs. 2–5 show the spatiotemporal patterns for $\xi \leq 4.8$, including coexistence steady state (see Fig. 2) given by

$$E^* \approx (0.6, 0.7, 1.2),$$

spatially homogeneous periodic solution(see Fig. 3), and spatially homogeneous periodic solution with one spatial frequency (see Fig. 4). By computations we obtain $\eta_2^H \approx 2.3253$, and Fig. 5 shows the spatially nonhomogeneous pattern near $(2,0)$-mode double-Hopf singularity. Interestingly, we still find that the indirect prey-taxis promotes the complexity of spatiotemporal patterns of the system, that is, when the sensitivity of the indirect prey-taxis increases, the spatiotemporal patterns of (1.4) will be more complicate.

If $\xi > 4.8$, i.e the sensitivity of the predator-taxis is large, based on Proposition 5.5-(ii) and by choosing $\xi = 10.5$, all other parameter are fixed as (5.10) and (5.11), spatiotemporal nonhomogeneous quasi-periodic pattern emerges, see Fig. 6. For any a fixes space location, we also simulate the evolution of the quasi-periodic solution over time, e.g. Fig. 7.

Finally, Figs. 8–9 exhibits the 3D phase trajectory in (N, P, S)-plane with a fixed spatial location, including the constant steady state, spatially homogeneous periodic solution with one spatial frequency, spatially nonhomogeneous periodic solution with two spatial frequencies and spatially nonhomogeneous quasi-periodic solution of (1.4), which correspond to the solutions sketched in Figs. 2–6, respectively.

6. Concluding remarks

We consider a general Gause–Kolmogorov-Type predator–prey model with direct predator-taxis and indirect prey-taxis. We prove that solutions exist globally and are uniformly bounded for bounded domains with a one-dimension and any taxis coefficient. Meanwhile, such results also hold under similar assumptions for the following more general predator–prey system in a one-dimension spatial domain:

$$\begin{cases} N_t = d_N \triangle N + \xi \nabla \cdot (N \nabla P) + f(N) - \phi(N, P), & x \in \Omega,\ t > 0, \\ P_t = d_P \triangle P - \eta \nabla \cdot (P \nabla S) + e\phi(N, P) - g(P), & x \in \Omega,\ t > 0, \\ S_t = d_S \triangle S + \alpha N - \beta S, & x \in \Omega,\ t > 0, \\ \frac{\partial N}{\partial \nu} = \frac{\partial N}{\partial \nu} = \frac{\partial N}{\partial \nu} = 0, & x \in \partial\Omega,\ t > 0, \\ N(x,0) = N_0(x) \geq 0, \quad P(x,0) = P_0(x) \geq 0, \quad S(x,0) = S_0(x) \geq 0, & x \in \Omega. \end{cases} \tag{6.1}$$

The global existence and uniformly boundedness for the cases of spatial dimension $n \geq 2$ perhaps can be proved as well if some conditions are restricted, it will be studies in the future investigation.

Moreover, we investigate the dependence of species success via the positive constant coexistence state in the system (1.4). Our results on success measures show that the species benefits from a decrease in the indirect prey-taxis sensitivity or the release rate

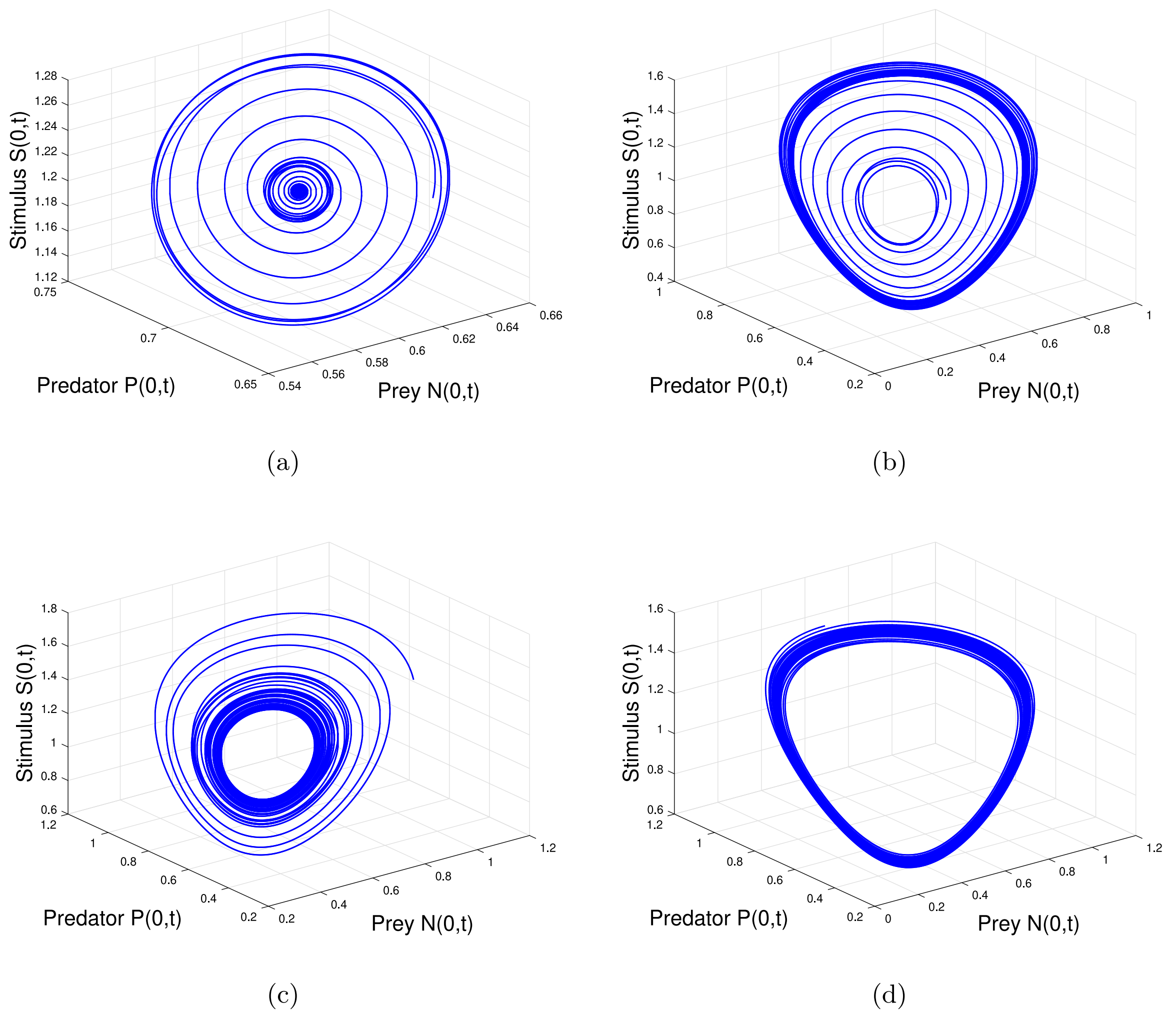

Fig. 8. For the same parameters as Figs. 3–6, fix the space location $x = 0$, graphs (a)–(d) show the 3D phase trajectory of Figs. 3–6, i.e. the solution of (1.4) converges to the constant steady state, spatially homogeneous periodic solution, spatially nonhomogeneous periodic solution with one spatial frequencies and spatially nonhomogeneous periodic solution with two spatial frequencies.

of stimulus, as well as an increase in the decay rate of stimulus. Increasing the direct predator-taxis sensitivity promotes the species success only when both the predator and prey diffuse fast.

Based on the existing results, by employing linear stability analysis, we prove Turing instability will not occur in the system (1.4) and establish the existence of Hopf and double-Hopf bifurcations, moreover, the stability of the constant steady state is further characterized. As well known, if the taxis is absent in the system, the constant steady state only can be destabilized through spatially homogeneous Hopf bifurcation, double-Hopf bifurcation cannot occur as well, this means complex spatialtemporal phenomena are difficult to emerge. Through religious bifurcation analyses, we find that as the indirect prey-taxis sensitivity increases, more complex and diverse spatiotemporal patterns can emerge in a system with indirect prey-taxis and direct predator-taxis, for example, spatially nonhomogeneous periodic patterns with different spatial frequencies, even spatially nonhomogeneous quasi-periodic patterns, see Figs. 2–6. It theoretically explains that the nonhomogeneous distribution of populations in the habitat, and the distribution changes periodically. Furthermore, if the system adopts a strong sensitivity of direct predator-taxis, the spatiotemporal pattern becomes more intricate, as shown in Fig. 6. This further illustrates that the cognitive movement between the predator and prey can cause the spatially heterogeneous distributions, even with a certain periodicity.

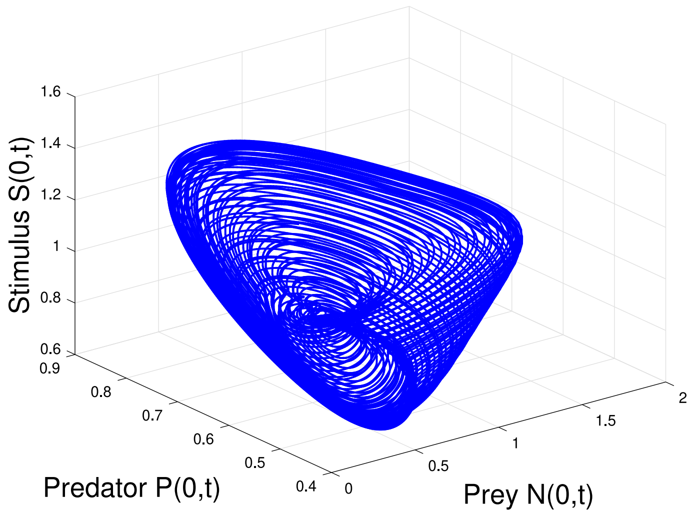

(a)

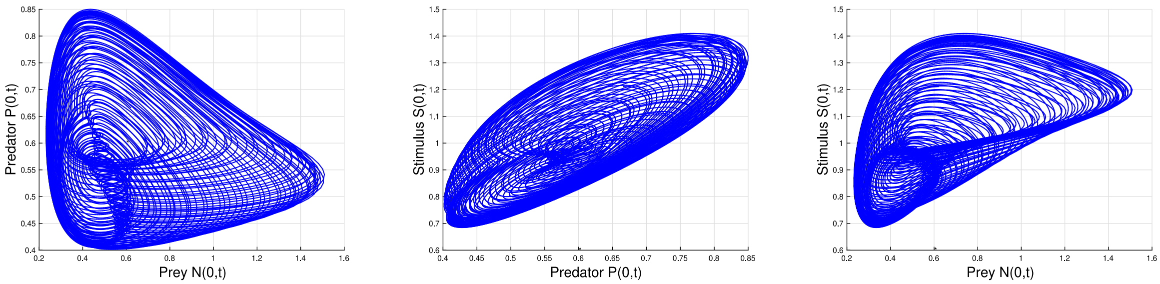

(b) Corresponding 2D projection trajectories in (N, P), (N, S), (P, S)-planes.

Fig. 9. For fixed space location $x = 0$, graphs show the phase trajectory of the spatially nonhomogeneous quasi-periodic solution of (1.4) in Fig. 6.

CRediT authorship contribution statement

Dongxu Geng: Put forward to the study object in this paper, Mathematical proofs and derivations, Writing – original draft, Revised the manuscript. **Hao Wang:** Put forward to the study object in this paper, Provided the idea of "measure of success", Polish our English writing for the whole manuscript, Revised the manuscript. **Weihua Jiang:** Provided beneficial mathematical suggestions and checked the results, Revised the manuscript. **Hongbin Wang:** Provided beneficial mathematical suggestions and checked the results, Revised the manuscript.

Declaration of competing interest

The authors declare that they have no known competing financial interests or personal relationships that could have appeared to influence the work reported in this paper.

Data availability

No data was used for the research described in the article.

Acknowledgments

The research of D.X. Geng, W. H. Jiang and H.B. Wang are partially supported by the National Natural Science Foundation of China (No. 11871176). The research of H. Wang is partially supported by the Natural Sciences and Engineering Research Council of Canada (Individual Discovery Grant RGPIN-2020-03911 and Discovery Accelerator Supplement Award RGPAS-2020-00090).

References

[1] Rosenzweig ML, Macarthur RH. Graphical representation and stability conditions of predator-prey interactions. Amer Nat 1963;97(895):209–23.
[2] Cui R, Shi J, Wu B. Strong allee effect in a diffusive predator-prey system with a protection zone, J. Differential equations 256 (2014). J Differential Equations 2014;256:108–29.
[3] Du Y, Shi J. Allee effect and bistability in a spatially heterogeneous predator–prey model. Trans Amer Math Soc 2007;359:4557–93.
[4] Yi F, Wei J, Shi J. Bifurcation and spatiotemporal patterns in a homogeneous diffusive predator-prey system. J Differential Equations 2009;246(5):1944–77.
[5] Medvinsky AB, Petrovskii SV, Tikhonova IA, Li BL. Spatiotemporal complexity of Plankton and fish dynamics. SIAM Rev 2002;44(3):311–70.
[6] Turing AM. The chemical basis of morphogenesis. Philos Trans R Soc B 1952;237:37–72.
[7] Segel LA, Jackson JL. Dissipative structure: an explanation and an ecological example. J Theoret Biol 1972;37(3):545–59.
[8] Wang H, Salmaniw Y. PDE guidance for cognitive animal movement. 2022, http://dx.doi.org/10.48550/arXiv.2201.09150.
[9] Shi J, Wang C, Wang H, Yan X. Diffusive spatial movement with memory. J Dynam Differ Equ 2020;32(2):979–1002.
[10] Shi Q, Shi J, Wang H. Spatial movement with distributed memory. J Math Biol 2021;82(4):1–32.
[11] Song Y, Wu S, Wang H. Spatiotemporal dynamics in the single population model with memory-based diffusion and nonlocal effect. J Differential Equations 2019;267(11):6316–51.
[12] Song Y, Shi J, Wang H. Spatiotemporal dynamics of a diffusive consumer-resource model with explicit spatial memory. Stud Appl Math 2022;148(1):373–95.
[13] Ainseba BE, Bendahmane M, Noussair A. A reaction–diffusion system modeling predator–prey with prey-taxis. Nonlinear Anal RWA 2008;9(5):2086–105.
[14] Cosner C. Reaction-diffusion-advection models for the effects and evolution of dispersal. Discrete Contin Dyn Syst 2014;34(5):1701–45.
[15] Lee JM, Hillen T, Lewis MA. Pattern formation in prey-taxis systems. J Biol Dyn 2009;3:551–73.
[16] Kareiva P, Odell G. Swarms of predators exhibit "preytaxis" if individual predators use area-restricted search. Amer Nat 1987;130:233–70.
[17] Wu S, Shi J, Wu B. Global existence of solutions and uniform persistence of a diffusive predator-prey model with prey-taxis. J Differential Equations 2016;260(7):5847–74.
[18] Wu S, Wang J, Shi J. Dynamics and pattern formation of a diffusive predator-prey model with predator-taxis. Math Models Methods Appl Sci 2018;28:2275–312.
[19] Othmer H, Stevens A. Aggregation, blowup, and collapse: The abc's of taxis in reinforced random walks. SIAM J Appl Math 1997;57(4):1044–81.
[20] Tao Y. Global existence of classical solutions to a predator-prey model with nonlinear prey-taxis. Nonlinear Anal RWA 2010;11(3):2056–64.
[21] Wang X, Wang W, Zhang G. Global bifurcation of solutions for a predator-prey model with prey-taxis. Math Methods Appl Sci 2015;38(3).
[22] Wang J, Wu S, Shi J. Pattern formation in diffusive predator-prey systems with predator-taxis and prey-taxis. Discrete Contin Dyn Syst Ser B 2021;26(3):1273–89.
[23] Arditi R, Tyutyunov Y, Morgulis A, Govorukhin V, Senina I. Directed movement of predators and the emergence of density-dependence in predator- prey models. Theor Popul Biol 2001;59(23):207–21.
[24] Tyutyunov Y, Titova L, Arditi R. A minimal model of pursuit-evasion in a predator–prey system. Math Model Nat Phenom 2007;2(4):122–34.
[25] Tyutyunov Y, Senina I, Arditi R. Clustering due to acceleration in the response to population gradient: A simple self-organization model. Amer Nat 2004;164(6):722–35.
[26] Chakraborty A, Singh M, Lucy D, Ridland P. Predator–prey model with prey-taxis and diffusion. Math Comput Model 2007;46(3–4):482–98.
[27] Tello JI, Wrzosek D. Predator–prey model with diffusion and indirect prey-taxis. Math Models Methods Appl Sci 2016;26:2129–62.
[28] Tyutyunov Y, Titova L, Senina I. Prey-taxis destabilizes homogeneous stationary state in spatial Gause–Kolmogorov-type model for predator–prey system. Ecol Complex 2017;31:170–80.
[29] Ahn I, Yoon C. Global well-posedness and stability analysis of prey-predator model with indirect prey-taxis. J Differential Equations 2019;268(8).
[30] Tyutyunov Y, Sen D, Titova L, Banerjee M. Predator overcomes the allee effect due to indirect prey-taxis. Ecol Complex 2019;39:100772.1–100772.16.
[31] Liang D, So WH, Zhang F, Zou X. Population dynamic models with nonlocal delay on bounded domains and their numerical computations. Differ Equ Dyn Syst 2003;11:117–39.
[32] Ahn I, Yoon C. Global solvability of prey–predator models with indirect predator-taxis. Z Angew Math Phys 2021;72(1).
[33] Mishra P, Wrzosek D. Repulsive chemotaxis and predator evasion in predato- rprey models with diffusion and prey-taxis. Math Models Methods Appl Sci 2022;32:1–42.
[34] Wu S. Global boundedness of a diffusive prey-predator model with indirect prey-taxis and predator-taxis. J Math Anal Appl 2022;507:125820.
[35] Amann H. Dynamic theory of quasilinear parabolic equations II. Differ Integral Equ 1990;3(1):13–75.
[36] Amann H. Function spaces, differential operators and nonlinear analysis. Teubner Texte Math 1993;133:9–126.
[37] Horstmann D, Winkler M. Boundedness vs. blow-up in a chemotaxis system. J Differential Equations 2005;215(1):52–107.
[38] Winkler M. Aggregation vs. global diffusive behavior in the higher-dimensional Keller–Segel model. J Differential Equations 2010;248(12):2889–905.
[39] Friedmann A. Partial differential equations of parabolic type. New York: Holt, Rinehart and Winston; 1964.
[40] Winkler M, Djie KC. Boundedness and finite-time collapse in a chemotaxis system with volume-filling effect. Nonlinear Anal 2010;72(2):1044–64.
[41] Nirenberg L. An extended interpolation inequality. Ann Sc Norm Super Pisa Cl Sci 1966;3(20):733–7.
[42] Wang J, Shi J, Wei J. Dynamics and pattern formation in a diffusive predator-prey system with strong Allee effect in prey. J Differential Equations 2011;251(4–5):1276–304.
[43] Liu Z, Shen Z, Wang H, Jin Z. Analysis of a diffusive SIR model with seasonality and nonlocal incidence of infection. SIAM J Appl Math 2019;79(6):2218–41.
[44] Alikakos ND. L^p Bounds of solutions of reaction-diffusion equations. Comm Partial Differential Equations 1979;4(8):827–68.
[45] Corrias L, Perthame B, Zaag H. L^p And L^∞ a priori estimates for some chemotaxis models and applications to the Cauchy problem (dynamics of spatio-temporal patterns for the system of reaction-diffusion equations). Kyoto Univ RIMS 2005;1416:105–19.
[46] Geng D, Wang H. Normal form formulations of double-Hopf bifurcation for partial functional differential equations with nonlocal effect. J Differential Equations 2022;309:741–85.